Volume 140 | Number 21 | 7 November 2015 | Pages 7033–7452

Analyst

www.rsc.org/analyst

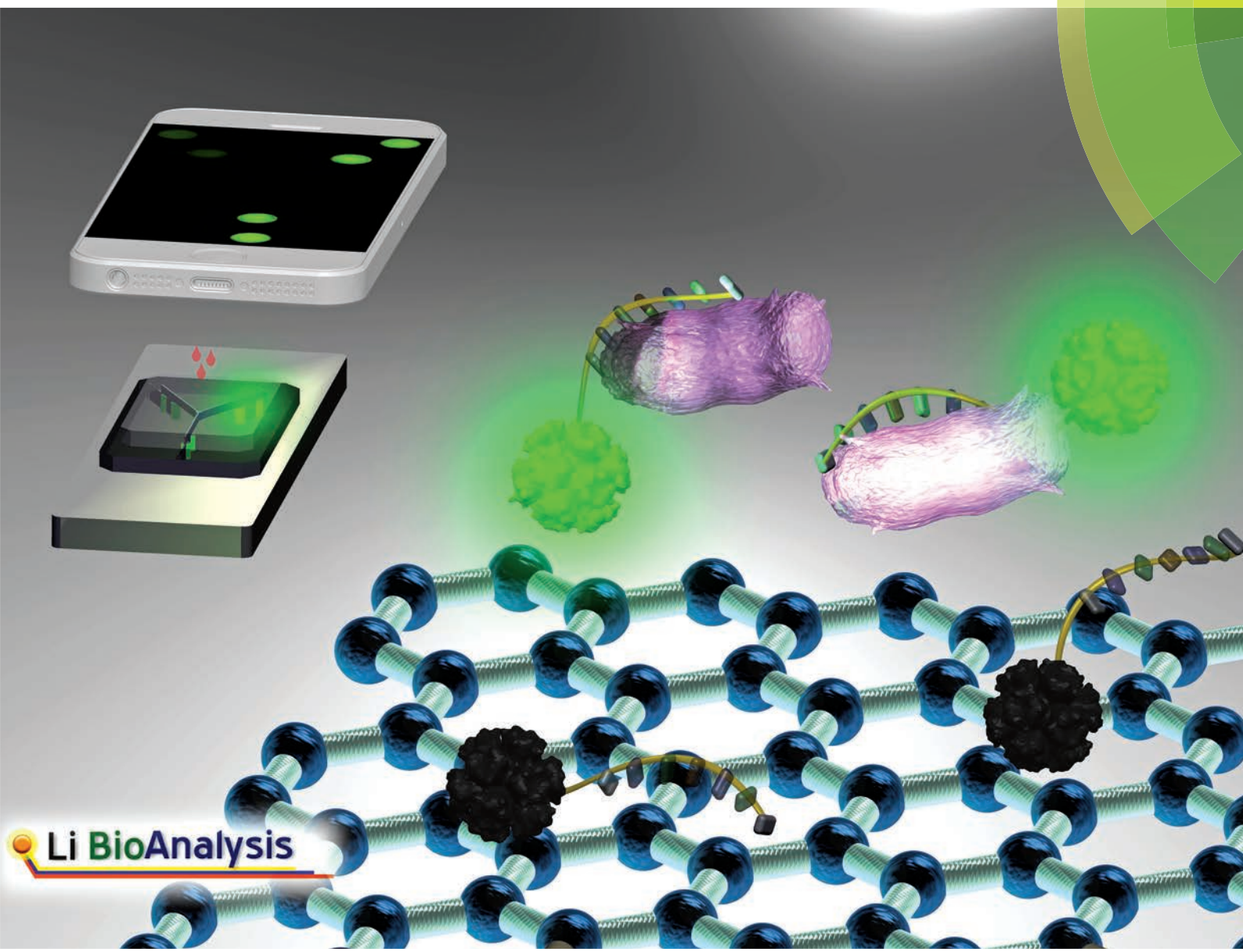

ISSN 0003-2654

ROYAL SOCIETY OF CHEMISTRY

CRITICAL REVIEW

XiuJun Li *et al.*

Biomarker detection for disease diagnosis using cost-effective microfluidic platforms

Analyst

CRITICAL REVIEW

View Article Online
View Journal | View Issue

Cite this: *Analyst*, 2015, **140**, 7062

Biomarker detection for disease diagnosis using cost-effective microfluidic platforms

Sharma T. Sanjay,[a] Guanglei Fu,[a] Maowei Dou,[a] Feng Xu,[b,c] Rutao Liu,[d] Hao Qi[e] and XiuJun Li*[a,f,g]

Received 21st April 2015,
Accepted 23rd June 2015

DOI: 10.1039/c5an00780a

www.rsc.org/analyst

Early and timely detection of disease biomarkers can prevent the spread of infectious diseases, and drastically decrease the death rate of people suffering from different diseases such as cancer and infectious diseases. Because conventional diagnostic methods have limited application in low-resource settings due to the use of bulky and expensive instrumentation, simple and low-cost point-of-care diagnostic devices for timely and early biomarker diagnosis is the need of the hour, especially in rural areas and developing nations. The microfluidics technology possesses remarkable features for simple, low-cost, and rapid disease diagnosis. There have been significant advances in the development of microfluidic platforms for biomarker detection of diseases. This article reviews recent advances in biomarker detection using cost-effective microfluidic devices for disease diagnosis, with the emphasis on infectious disease and cancer diagnosis in low-resource settings. This review first introduces different microfluidic platforms (*e.g.* polymer and paper-based microfluidics) used for disease diagnosis, with a brief description of their common fabrication techniques. Then, it highlights various detection strategies for disease biomarker detection using microfluidic platforms, including colorimetric, fluorescence, chemiluminescence, electrochemiluminescence (ECL), and electrochemical detection. Finally, it discusses the current limitations of microfluidic devices for disease biomarker detection and future prospects.

1. Introduction

As a disease attacks a person, physiological signals that represent the biological state of the person change in response to the status of the disease. A biomarker is a characteristic that is objectively measured and evaluated as an indicator of normal biological processes, pathogenic processes, pharmacologic responses to therapeutic intervention or any measurable diagnostic indicator for assessing the risk or the presence of a disease.[1] It can include mRNA expression profiles, circulating DNA and tumor cells, proteins, proteomic pattern, lipids, metabolites, imaging methods or electrical signals.[2–5] These signals/biomarkers may be obtained from sources such as urine, blood and tissues. Disease biomarker detection that is desired to be accurate, relatively noninvasive and easy to perform, even in point-of-care (POC) settings, can improve the screening, diagnosis, prognosis and recovery on treatment of various diseases.

Acute infectious diseases caused by pathogenic organisms such as bacteria, viruses, fungi and parasites have been a major cause of global death and high disability rates throughout the human history.[6,7] In developing nations, even curable infectious diseases pose a great threat to patients due to lack of affordable diagnosis.[8] According to a global report on infectious disease of poverty (2012) by World Health Organization (WHO), each year infectious diseases kill 3.5 million people, mostly the poor and young children who live in low and middle-income countries.[9] Over 95% of deaths by infectious disease are due to the lack of proper diagnosis and treatment, and difficulty in accessing adequate healthcare infrastructures.[8] Along with infectious diseases, cancer, the uncontrolled growth of abnormal cells which can spread and invade other parts of the body through the blood and lymph system, also

[a]*Department of Chemistry, University of Texas at El Paso, 500 West University Ave, El Paso, Texas 79968, USA. E-mail: xli4@utep.edu*
[b]*Bioinspired Engineering and Biomechanics Center (BEBC), Xi'an Jiaotong University, Xi'an 710049, P. R. China*
[c]*MOE Key Laboratory of Biomedical Information Engineering, School of Life Science and Technology, Xi'an Jiaotong University, Xi'an 710049, P. R. China*
[d]*School of Environmental Science and Engineering, China, America CRC for Environment & Health, Shandong Province; Shandong University, 27# Shanda South Road, Jinan 250100, P. R. China*
[e]*School of Chemical Engineering and Technology, Tianjin University, Tianjin, 300072, P. R. China*
[f]*Biomedical Engineering, University of Texas at El Paso, 500 West University Ave, El Paso, Texas 79968, USA*
[g]*Border Biomedical Research Center, University of Texas at El Paso, 500 West University Ave, El Paso, Texas 79968, USA*

figures among the leading causes of death worldwide with 8.2 million deaths in 2012, according to WHO.[10] Annual cancer cases are expected to rise from 14 million in 2014 to 22 million within the next 2 decades. Similar to infectious diseases, high incidence of cancer occurs in developing nations. According to WHO, 8 million (57%) new cancer cases, 5.3 million (65%) cancer deaths and 15.6 million (48%) 5-year prevalence cancer cases occurred in less developed regions.[11]

Infectious diseases and cancer along with other diseases are mostly diagnosed by biomarker detection in laboratories using conventional tests such as enzyme linked immunosorbent assay (ELISA), immunofluorescence, western blotting, immunodiffusion, polymerase chain reaction (PCR), flow cytometry and a wide range of other techniques.[12–14] However, most of these assays are complex, take hours for completion, consume large volumes of samples and reagents, and require bulky and expensive instruments limiting their applications in rural areas and developing nations. Therefore, simple, low-cost, portable diagnostic devices and methods, especially POC diagnostic devices that offer great potential to detect and monitor diseases, even at resource-limited settings are absolutely essential. Development of POC devices for simple, timely and early disease diagnosis can prevent the spread of infectious diseases, and decrease cancer fatality, as many cancer patients (including breast, colorectal, oral and cervical) have high chance to be cured if detected early and treated adequately. WHO has developed a list of general characteristics that make a diagnostic test appropriate for resource-limited sites, abbreviated as ASSURED, and includes: Affordable by those at risk, Sensitive, Specific, User-friendly, Rapid treatment and robust use, Equipment-free and finally Delivered to those who need it.[15]

Microfluidics technology possesses remarkable features for simple, low-cost, and rapid disease diagnosis, such as low volumes of reagent consumption, fast analysis, high portability along with integrated processing and analysis of complex biological fluids with high sensitivity for health care application.[16–22] An enormous number of microfluidic devices have been developed for biomedical applications.[23–29] These devices enable on-chip POC diagnosis and real-time monitoring of diseases from a small volume of body fluids. These microfluidic devices may act as a bridge to improve the global health care system with high efficiency and sensitivity, especially for remote areas with low-resource settings, such as the underdeveloped and developing countries, in home health care setting, and in emergency situations. Because of all these significant features, numerous microfluidic devices have been developed for the biomarker detection in disease diagnosis, which includes different types of cancers[30–32] from colorectal carcinoma[33,34] and hepatocellular carcinoma[32] to ovarian cancer[33,35] and prostate cancer,[36,37] different types of infectious diseases from food-borne pathogen[38] and Hepatitis B[39] to meningitis[40,41] and dengue virus,[42] and other diseases from cardiovascular disease[43,44] to Alzheimer's diseases.[45] These microfluidic platforms include glass,[21,46,47] polydimethylsiloxane (PDMS),[45,48,49] poly(methyl methacrylate) (PMMA),[36,50,51] poly(cyclic olefin),[52,53] and paper-based[23,54–59] and hybrid devices.[36,60,61]

This article reviews recent advances of biomarker detection for disease diagnosis using microfluidic techniques. It first introduces different microfluidic POC platforms used for disease biomarker detection with a brief introduction of their common fabrication techniques. Because of their ease of fabrication, cost-effective characteristics, and broad applications in disease diagnosis, this article mainly focuses on cost-effective microfluidic platforms such as polymer (*e.g.* PDMS and PMMA) and paper-based microfluidic platforms. Next, it highlights various detection strategies for disease biomarker detection using microfluidic devices, including colorimetric, fluorescence, chemiluminescence, electrochemiluminescence (ECL), and electrochemical detection. Lastly, we briefly discuss the future trends in this field. Although microfluidic platforms have great potential for the diagnosis of a broad range of diseases, this article emphasizes the applications of microfluidic devices in infectious diseases and cancer.

Sharma T. Sanjay

Sanjay Sharma Timilsina from Nepal received his master's and bachelor's degrees in biotechnology from Bangalore University, Bangalore, India in 2010 and 2012 respectively. He is currently a Ph.D. student with Dr XiuJun (James) Li in the Department of Chemistry at the University of Texas at El Paso, TX, USA. His research interest is focused on low-cost diagnosis of infectious diseases on microfluidic platforms. He is also interested in 3D cell culture and bioanalysis.

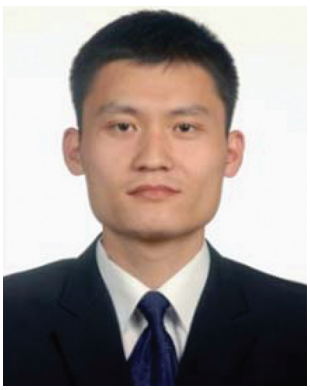

Guanglei Fu

Guanglei Fu received his Ph.D. in biomedical engineering in 2013 from Harbin Institute of Technology, China. Currently, he is a postdoctoral research fellow in Dr XiuJun (James) Li's Lab in the Department of Chemistry at the University of Texas at El Paso (UTEP), USA. His current research interest is focused on nanobiosensing and nanomedicine.

2. Microfluidic platforms for biomarker detection

In the early stage of microfluidics, microfluidic devices were predominantly made with methods borrowed from microelectronics field and involved materials such as glass, quartz or silicon. Silicon and glass are more expensive and less flexible to work with, as compared to polymers (*e.g.* PMMA and PDMS). Most of them have good optical properties similar to glass, but their fabrication (*e.g.* soft lithography[62–64]) does not have stringent requirements on cleanroom facility, which makes polymer-based microfluidic devices widely used. Within the past few years, paper-based microfluidic devices have debuted as a lower-cost microfluidic platform.[19,65,66] The choice of material depends on the research application, detection system, fabrication facility, cost and other factors such as resistance to different chemicals, thermal conductivity, dielectric strength and sealing properties. This section mainly aims to give a general introduction of various cost-effective microfluidic platforms used for disease biomarker detection. Since the focus of this article is not to review recent fabrication techniques, only common fabrication techniques and their recent advances are briefly described. A few other review articles have described more details of fabrication methods for different microfluidic platforms.[67–69]

2.1 PDMS microfluidic platforms

PDMS is one of the most widely used elastomers for microfluidic devices as it is optically transparent, elastic, and cures at low temperature. It can seal with itself and a range of other materials after being exposed to air plasma. The ease and low cost of fabrication and the ability to be cast in high resolution add to its advantages. In contrast to other thermoplastic materials, PDMS is gas permeable, making it compatible for cell culture. Although PDMS is one of the most widely used cost-effective microfluidic platforms, there are some limitations of PDMS as well. PDMS swells in organic solvents and low molecular weight organic solutes. It cannot withstand high temperature and the mechanical resistance is quite low. There are different methods available for the fabrication of PDMS devices including soft lithography, casting, injection molding, imprinting, hot embossing, laser ablation and others.[22,62,63]

Soft lithography is the most widely used method for PDMS fabrication. Soft lithography can start with the creation of a photomask on a transparency film. The resolution of transparency is >20 μm as compared to a chrome mask ~500 nm.[71] A photoresist is then added to the silicon wafer, and exposed to UV light through the photomask to produce a positive relief of photoresist on a silicon wafer (master). Masters can also be fabricated by techniques like etching in silicon and electroforming metal. Channels in PDMS can be formed by replica molding once a master is fabricated. The cured PDMS replica can be bonded with another flat layer of PDMS, glass or other materials to form a closed system. Based on soft lithography, Kung *et al.*[70] demonstrated a novel method for fabricating 3D high aspect ratio PDMS microfluidic networks with a hybrid stamp. Fig. 1 shows the schematic of fabrication process flow. An SU8 master is treated with trichloro (1*H*,1*H*,2*H*,2*H*-perfluorooctyl)silane (PFOCTS) to facilitate subsequent demolding. An uncured PDMS mixture is then poured on the master followed by pressing against the hybrid stamp. Then, the casted PDMS film is peeled off from the master since it tends to adhere to the hybrid stamp, as there is less PFOCTS on the hybrid stamp. Afterwards, the PDMS film is transferred and bonded with glass/silicon by oxygen plasma treatment, followed by the removal of the supporting PDMS, the polystyrene plastic plate and residual PDMS. Finally, the stacking process is repeated to complete the 3D fabrication. They showed that multilayer 3D PDMS structures could be constructed and bonded between two hard substrates. As an example, they fabricated a microfluidic 3D deformable channel by sandwiching two PDMS membranes (20 μm wide and 80 μm tall) between two glass

Maowei Dou

Maowei Dou received his B.E. and M.E. degrees from the College of Chemistry and Chemical Engineering at Ocean University of China, China, in 2009 and 2012, respectively. He is currently a Ph.D. student in the Department of Chemistry at the University of Texas at El Paso, USA. His research is focused on low-cost infectious disease diagnosis on hybrid microfluidic platforms.

Feng Xu

Feng Xu received his Ph.D. in 2008 from Cambridge University. During 2008–2011, Dr Xu worked as a research fellow at Harvard Medical School and Harvard-MIT Health Science & Technology (HST). Currently, Dr Xu is a full professor and a vice dean at the School of Life Science & Technology, and also Founding director of Bioinspired Engineering & Biomechanics Center, Xi'an Jiaotong University, China. Dr Xu's current research focuses on bio-thermo-mechanics, engineering of cell microenvironment, and point-of-care technologies.

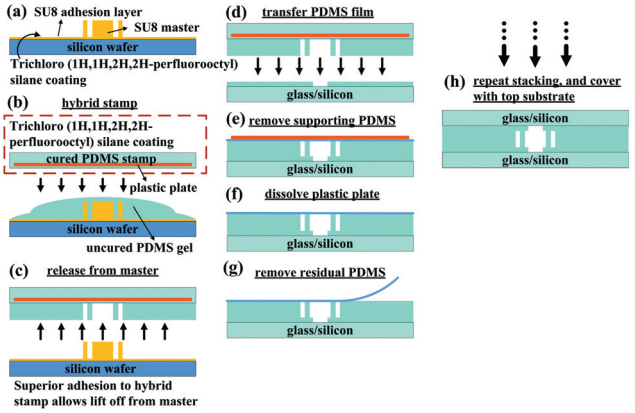

Fig. 1 Fabrication schematic of 3D high aspect ratio PDMS microfluidic networks using a plastic plate embedded hybrid stamp. Reproduced with permission from Royal Society of Chemistry.[70]

substrates. This 3D fabrication method could be applied in electrokinetics, optofluidics, inertial microfluidics, and other fields where the shape of the channel cross-section is significant in device physics. Comina *et al.*[72] described another method for fabrication of 3D PDMS devices using templates printed with a commercial micro-stereo lithography 3D printer with a resolution of 50 μm. The process eliminates the need for clean room facilities and repeated photolithographic steps required for templates with different thicknesses. They reported that the templates are reusable and can be fabricated within 20 min, with an average cost of 0.48 US$.

2.2 Thermoplastic microfluidic platforms

Thermoplastics are also being used as a substitute for glass and silicon as the microfluidic platform due to their chemical and mechanical properties. Thermoplastic devices are economical for mass production and are compatible with most chemical reagents and biological assays. Several kinds of thermoplastics have been used such as PMMA (*i.e.* acrylic), polycarbonate, polyester and polyvinylchloride (PVC), because of their low-cost, desirable optical properties and ease of fabrication. They offer better performances than PDMS under mechanical stress. They don't require long fabrication and curing time. These thermoplastic devices can be fabricated easily by cutting the pattern using a CO_2 laser cutter followed by bonding with an adhesive or heat to form 3D devices. Multilayered devices can be completely fabricated and become ready for testing in as little as several hours.[73] Cassano *et al.*[74] used vacuum bagging for thermal bonding of thermoplastic microfluidic devices. Vacuum bagging completely eliminates time constrains resulting from using solvents, adhesives, or surface treatments. With fabrication technologies including hot embossing or imprinting,[75,76] laser ablation,[77] injection molding[78] and soft lithography, dimensions of plastic microchannels can be achieved in the range of 15–30 μm. Recently, simple methods have been developed for rapid prototyping of thermoplastic microfluidic platforms. For example, Roy *et al.*[79] reported a rapid prototyping technique for fabrication of a multilayer microfluidic device using styrenic thermoplastic elastomer (TPE). They established a proof of principle for valving and mixing with three different grades of TPE using an SU-8 master mold. Miserere *et al.*[80] proposed a strategy for the fabrication of flexible thermoplastic microdevices based on the lamination process. A low-cost laminator can be used from master fabrication to microchannel sealing. They demonstrated the process using Cyclo-olefin Copolymer (COC). Rahmanian *et al.*[81] described rapid desktop manufacturing of sealed thermoplastic microchannels. Patterning was achieved by simply drawing the desired microchannel pattern onto the

Rutao Liu

Rutao Liu received his B.S. degree from Qufu Normal University in 1996 and his M.S. degree from Shandong University in 1999 and Ph.D. degree in analytical chemistry from Shandong University in 2002. Then he did his postdoctoral research at Albert Einstein College of Medicine, Yeshiva University with Dr Mark R. Chance. Afterward, he joined Shandong University as a professor. His current research interests include Environmental pollution monitoring and health. He has published more than 110 scientific research papers.

XiuJun Li

XiuJun (James) Li received his Ph.D. in bioanalytical chemistry in 2008 from Simon Fraser University, Canada, and then moved to the University of California Berkeley with Dr Richard Mathies and to Harvard University with Dr George Whitesides for his postdoctoral research from 2009 to 2011, as a NSERC Postdoctoral Fellow.

Currently, he is a tenure-track Assistant Professor in the Department of Chemistry, Border Biomedical Research Center at the University of Texas at El Paso (UTEP), USA. His current research interest is centered on bioanalysis and bioengineering using microfluidic lab-on-a-chip and nanobiosensing, including low-cost disease diagnosis, hybrid microfluidic devices, single-cell analysis and 3D cell culture.

polymer surface using a suitable ink as a masking layer, followed by exposure to solvent vapor to yield a desired depth. The channels were then permanently sealed through solvent bonding of the microchannel chip to a mating thermoplastic substrate. Among these various fabrication methods, two of the most widely used fabrication techniques in the field of microfluidic biomarker detection are discussed in brief in this review.

2.2.1 Hot embossing. The hot embossing[75,76] or imprinting is an established method to fabricate microchannels in common polymers such as polystyrene (PS), polyethylene terephthalate glycol (PETG), PMMA, PVC, and polycarbonate. Silicon stamps are the more commonly used embossing tools for the fabrication of these polymeric microfluidic devices. A typical hot embossing setup consists of a force frame, which delivers the embossing force *via* a spindle and a T-bar to the boss or the embossing master. The microstructures are then transferred from the master to the polymer by stamping the master into the polymer by heating above its glass transition temperature (T_g) under vacuum.[75] Alternatively, polymer devices can be imprinted at room temperature with elevated pressure. The master structure is pressed into the thermoplastic substrate with a force (*e.g.* 20–30 kN in the case of PMMA or PC) depending on the type and size of the substrate along with the feature to be imprinted.[75] Finally, the master and the substrate are isothermally cooled to a temperature just below T_g and then separated. The resulting plastic microchannel dimensions are the exact mirror image of the silicon stamp when devices are hot embossed.

2.2.2 Laser ablation. Laser ablation[77,82] is also one of the rapid prototyping methods for microfluidic devices. In this technique, the polymer is exposed to a high intensity laser beam, which evaporates the material at the focal point by photo-degradation or thermal-degradation or a combination of the two. A pulsed laser is typically used, so that each laser shot will ablate a defined amount of material, depending on the material type and absorption properties, laser intensity, wavelength and number of passes made across the channel. This process leads to the rough surface of the laser-ablated microchannels and have a rippled appearance, which depends upon the absorption of the polymer at excimer wavelength. Very high temperature is reached during ablation and particles are ejected from the substrate creating a void, with small particulates on the surface of the substrate material, while other decomposition products become gases (carbon dioxide and carbon monoxide). Laser ablation may be achieved by two ways. A polymer substrate can be exposed to a laser through a mask. A mask is usually made from the material that does not have significant absorption at the laser wavelength used. In the mask-less process, a polymer substrate is placed on a movable stage and either the focused laser beam or the substrate is moved across in the x and y direction as defined in the desired pattern.

2.3 Paper-based microfluidic platforms

Paper is a thin sheet of material that is generally produced by pressing together cellulosic or nitrocellulose fibers.[65] Paper can transport liquids *via* the capillary effect without the assistance of external forces. Fabrication of paper-based devices is simple and does not require the use of clean-room facilities. Paper has good stackability, which allows the formation of 3D structures for complex assays. The high surface to volume ratio provided by the macroporous structure in paper improves the immobilization of protein and DNA biomarkers, allowing fast detection. Paper-based microfluidic devices can be fabricated both in 2D and 3D for either horizontal or vertical flow.[68] Fabrication of the paper-based devices can be subdivided into two categories: (i) construction of hydrophobic barriers, and (ii) two-dimensional cutting.

2.3.1 Constructing hydrophobic barriers. One of the most widely used methods to prepare paper-based analytical devices (μPADs) is to construct hydrophobic barriers in the hydrophilic paper matrix. In this way, reagents and analytes can be made to flow in a certain path preventing mixing and spreading across the surrounding paper surface and achieve multiplexed assays without the issue of cross contamination. Hydrophobic barriers can be created on paper through either a physical deposition[83] or a chemical modification method.[84] A number of different fabrication methods have been developed to fabricate μPADs, such as fast photolithography,[85,86] wax-based fabrication techniques,[83,87] printing photolithography,[88] PDMS printing,[89] saline UV/O_3 patterning,[90] flexographic printing,[91] and alkenyl ketene dimer (AKD) printing.[84] Examples of wax-based fabrication include wax screen-printing,[87] wax dipping,[92] and wax printing.[83] In wax screen-printing,[87] solid wax is rubbed through a screen onto paper filters. The printed wax is then melted into paper so that the melted wax diffuses into paper to form hydrophobic barriers using a hot plate. In wax dipping,[92] an ironmould is first prepared by the laser cutting technique. The designed pattern is then developed into paper by transferring the pattern mould (sealed by magnets) into molten wax. Wax printing, in which the designed pattern is directly printed on paper using a solid ink (or wax) printer,[93] is considered to be one of the most promising and attractive wax-based methods, due to its low cost and high potential for massive production. After printing, the wax-printed paper is incubated in an oven so that the melted wax from the paper surface can penetrate into paper to form well-defined microchannels across the whole thickness of the paper-based device owing to the porous structure of the filter paper. The time required for the patterned wax on paper to penetrate through depends on the temperature used (5 min at 110 °C, 30 s at 130 °C) and the wax-patterned paper is stable when stored under 60 °C.[83] In 2014, Sameenoi *et al.*[94] reported one-step polymer screen-printing for microfluidic paper-based devices. In this process, a polystyrene solution that is applied through the screen penetrates through the paper to form a 3D hydrophobic barrier, defining a hydrophilic analysis zone. The smallest hydrophilic channel and hydrophobic barrier obtained was found to be 670 ± 50 μm and 380 ± 40 μm, respectively. Among these fabrication methods, photolithography and wax printing are widely used. Wax is inexpensive and non-toxic.[83,87,92] Recently, paper/polymer hybrid devices

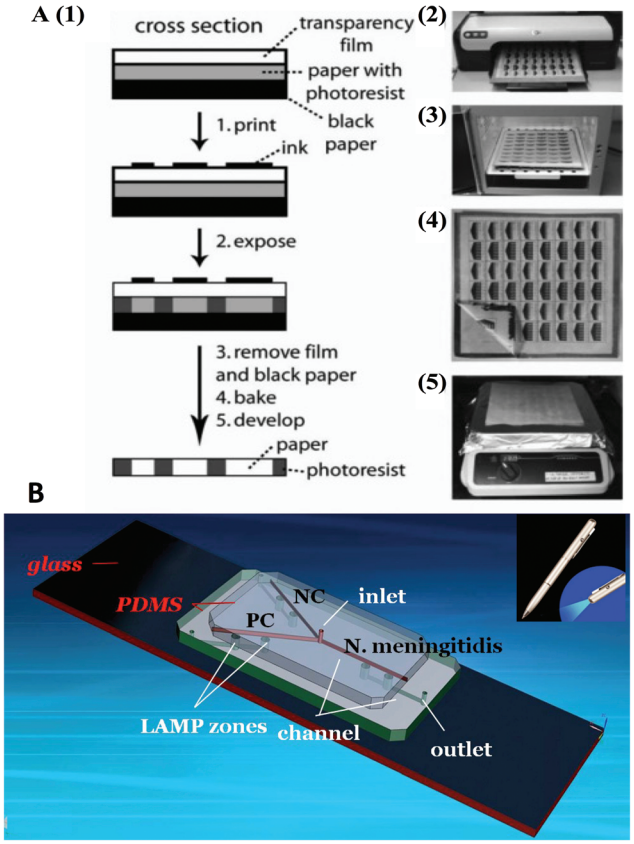

Fig. 2 Paper-based and its hybrid microfluidic platforms. (A) FLASH fabrication for paper-based microfluidic devices. (1) Schematic of the method. (2)–(5) FLASH fabrication procedures. Reproduced with permission from Royal Society of Chemistry.[86] (B) A PDMS/paper hybrid chip for instrument-free diagnosis of infectious diseases using a UV light pen. Reproduced with permission from American Chemical Society.[41]

have been developed (Fig. 2B), but their fabrication methods is mainly derived from a combination of paper-based and polymer microfluidic device fabrication techniques.[41,95]

FLASH (Fast Lithographic Activation of SHeets). One of the most widely used fabrication technology for constructing hydrophobic barriers in paper-based devices is photolithography or FLASH.[86] Chromatography paper is the commonly used substrate. FLASH requires a UV lamp, a printer and a hotplate along with a photoresist such as SU-8 and other organic solvents. Fig. 2A shows the procedures. In this technique[86] a photoresist is first poured onto a piece of paper and spread evenly and baked on a hotplate at 130 °C for 5–10 min to evaporate propylene glycol monomethyl ether acetate (PGMEA) from the photoresist. Then, the paper is covered with a photomask and exposed to UV light. After incubation in an oven, the chromatography paper is washed in acetone, followed by rinsing with isopropyl alcohol. After drying, the paper-based device is ready to use.

2.3.2 Two-dimensional cutting. Another way to create a paper-based microfluidic device is 2D cutting. Paper channels are cut through computer controlled *X*–*Y* knife plotters or CO_2 laser cutters, and then fixed to suitable plastic cassettes to form hybrid devices.[41,96] Nitrocellulose, conventional photocopy paper or chromatography paper can be used. Thuo *et al.*[97] described the use of embossing and a "cut-and-stack" method to develop microfluidic devices from omniphobic paper. They demonstrated that fluid flow in these devices was similar to open-channel microfluidic devices and cut layer generated 3D systems.

3. Biomarker detection methods for disease diagnosis using microfluidic devices

Wide ranges of detection methods have been employed for the detection of a number of disease biomarkers in microfluidic devices, as summarized in Table 1. Colorimetric, fluorescence and electrochemical detection remain the most widely used ones. Nevertheless, detection mechanisms such as chemiluminescence, electrochemiluminescence and other detection mechanisms have also been applied to disease biomarker detection.

3.1 Colorimetric detection

Colorimetric detection is generally carried out based on the color change of the detection system resulting from chemical/biochemical reactions between target analytes and colorimetric probes.[98] The major advantage of the colorimetric assay is that it doesn't rely on the bulky off-chip detection system, thus allowing naked-eye-based readout methods.[99] Therefore, colorimetric detection has attracted increasing research interest in the biomedical field especially for disease diagnosis due to its unique advantages for POC detection of infectious diseases.[100–103] The summary in Table 1 shows that colorimetric detection is less widely used in cancer biomarker detection.

Many researchers have made incredible advances in the field of colorimetric detection methods. Wide ranges of biomolecules from protein biomarkers for infectious diseases to glucose and nucleic acids have been studied using colorimetric detection. For instance, Yu *et al.*[39] reported a PDMS microfluidic chip for ELISA. The PDMS platform was modified with dextran to increase the hydrophilicity and to covalently immobilize proteins on the surface of PDMS. The colorimetric immunoassay in the modified PDMS microfluidic device was used to simultaneously detect multiple important biomarkers, interleukin-5 (IL-5, a biomarker for bronchial asthma), hepatitis B surface antigen (HBsAg, a biomarker for Hepatitis B virus) and immunoglobulin G (IgG, a biomarker for Neuromyelitis optica). 3,3′,5,5′-Tetramethylbenzidine (TMB) was used as the substrate for horseradish peroxidase (HRP) labelled secondary antibody. The chip allowed reaching a limit of detection (LOD) of 100 pg mL^{-1} and a dynamic range of 5 orders of magnitude. Covalent immobilization of protein can increase the specificity and sensitivity of the device. Yu *et al.*[104]

Table 1 Summary of biomarker detection using microfluidic platforms

	Specific disease	Biomarkers	LOD	Detection method	Microfluidic platform	Ref.
Cancer	Colorectal carcinoma	CEA	250 fM	Fluorescence	PDMS	122
		CEA	3.5 ng mL^{-1}	Fluorescence	PDMS	124
		CEA	0.01 ng mL^{-1}	Electrochemical	Paper	31
		CEA	0.01 ng mL^{-1}	Electrochemical	Paper	33
		CEA	0.05 ng mL^{-1}	Chemiluminescence	Paper	32
		CEA	0.02 ng mL^{-1}	Chemiluminescence	Paper	140
		CEA	0.5 ng mL^{-1}	ECL	Paper	147
		CEA	0.8 pg mL^{-1}	ECL	Paper	34
		CEA	1.25 ng mL^{-1}	SAW	PDMS	48
		CEA	0.3 pg mL^{-1}	Electrochemical	Paper	131
		CEA	1.7 pg mL^{-1}	Colorimetric	Paper	111
	Hepatocellular carcinoma	AFP	250 fM	Fluorescence	PDMS	122
		AFP	0.01 ng mL^{-1}	Electrochemical	Paper	31
		AFP	1 pg mL^{-1}	Electrochemical	PMMA	133
		AFP	0.06 ng mL^{-1}	Chemiluminescence	Paper	32
		AFP	1 ng mL^{-1}	Chemiluminescence	Paper	140
		AFP	0.15 ng mL^{-1}	ECL	Paper	147
		AFP	3.9 ng mL^{-1}	Fluorescence	PDMS	124
		AFP	0.2 fg/chip	Fluorescence	PDMS	123
		AFP	1.7 pg mL^{-1}	Colorimetric	Paper	111
	Ovarian cancer	CA-125	0.05 ng mL^{-1}	Electrochemical	Paper	31
		CA-125	0.2 mU mL^{-1}	Electrochemical	Paper	33
		CA-125	0.33 ng mL^{-1}	Chemiluminescence	Paper	32
		CA-125	0.6 U mL^{-1}	ECL	Paper	147
		CA-125	0.0074 U mL^{-1}	ECL	Paper	35
	Prostate cancer	PSA	0.23 pg mL^{-1}	Electrochemical	PDMS	49
		PSA	100 fg mL^{-1}	ECL	PMMA/PDMS	36
		PSA	1 pg mL^{-1}	ECL	Paper	34
		PSA	100 pg mL^{-1}	LSPR	POEGMA/glass	37
		PSA	3.2 ng mL^{-1}	Colorimetric	PMMA	108
		PSA	0.5 pM	Fluorescence	PNIPAAm	125
		PSA	100 pg mL^{-1}	ECL	POEGMA/glass	37
		IL-6	0.30 pg mL^{-1}	Electrochemical	PDMS	49
		IL-6	10 fg mL^{-1}	ECL	PMMA/PDMS	36
	Pancreatic cancer	CA-199	0.17 U mL^{-1}	ECL	Paper	147
		CA-199	0.0055 U mL^{-1}	ECL	Paper	148
		CA-199	0.06 U mL^{-1}	Chemiluminescence	Paper	140
	Breast cancer	CA153	0.05 ng mL^{-1}	Electrochemical	Paper	31
		CA153	0.4 U mL^{-1}	Chemiluminescence	Paper	140
	Human acute leukemia	HL-60	350 cells mL^{-1}	Electrochemical	Paper	55
		CCL-119	30 cells per 3 μL	Chemiluminescence	PDMS	142
	Renal cancer carcinoma	AQP1	24 pg mL^{-1}	LSPR	Paper	154
	Bladder cancer	APOA1	9.16 ng mL^{-1}	Fluorescence	PDMS	120
		TNF	3.1 pg mL^{-1}	Fluorescence	Cyclo-olefin	116
		TNF	1000 copies per 4.7 nL	Fluorescence	PDMS	115
Infectious disease	Hepatitis B	HBsAg	100 pg mL^{-1}	Colorimetric	PDMS	39
	Pseudorabies virus	Nucleic acid	10 fg μL^{-1}	Colorimetric	PDMS	106
	Dengue virus	IgG/IgM	21 pg mL^{-1}	Fluorescence	PDMS	42
	Meningitis	ctrA gene	3 copies per LAMP zone	Fluorescence	PDMS/paper hybrid	41
	Food-borne disease	SEB	0.01 ng mL^{-1}	Chemiluminescence	Polycarbonate	143
	Food-borne pathogens	*S. enterica* (aptamer)	61 cfu mL^{-1}	Fluorescence	PDMS/paper hybrid	95
		S. aureus (aptamer)	800 cfu mL^{-1}	Fluorescence	PDMS/paper hybrid	95
		E. coli	5×10^5 cells per mL	Chemiluminescence	PMMA	51
		C. jejuni	1×10^5 cells per mL	Chemiluminescence	PMMA	51
		IgG	3.9 fM	Electrochemical	Paper	130
		IgG	10 pg mL^{-1}	Colorimetric	PDMS	104

Table 1 *(Contd.)*

	Specific disease	Biomarkers	LOD	Detection method	Microfluidic platform	Ref.
Other diseases	Diabetics	Glucose	0.5 mM	Colorimetric	Paper	54
		Glucose	0.35 mM	Electrochemical	Paper	136
	Thyroid dysfunction	Human thyroid stimulating hormone	68 pg mL^{-1}	Chemiluminescence	PDMS/glass	141
	Cardiovascular disease	cTnI	5 amol/30 μL	Electrochemical	PDMS	134
		cTnI	25 pg mL^{-1}	Electrochemical	Vacrel® 8100 photoresist	43
		cTnI	0.51 ng mL^{-1}	Colorimetric	PMMA	105
		cTnI	24 pg mL^{-1}	Fluorescence	PMMA	50
		CRP	307 amol per 30 μL	Electrochemical	PDMS	134
		CRP	0.30 ng mL^{-1}	Colorimetric	PMMA	105
		NT-proBNP	0.03 ng mL^{-1}	Electrochemical		135
		NT-proBNP	0.24 ng mL^{-1}	Colorimetric	PMMA	105
	Alzheimer's disease	ApoE	12.5 ng mL^{-1}	Electrochemical	PDMS	45
	Bronchial asthma	IL-5	100 pg mL^{-1}	Colorimetric	PDMS	39
	Neuromyelitis optica	IgG	100 pg mL^{-1}	Colorimetric	PDMS	39
		Uric acid	0.52 mM	Electrochemical	Paper	136
		Uric acid	8.1 ppm	Colorimetric	Paper	112
		Lactate	1.76 mM	Electrochemical	Paper	136

described the UV-curable epoxy resin based microarray and immunoassay device, using PDMS mold, and taking advantages of the functional epoxide group for efficient protein immobilization. The LOD was 10 pg mL^{-1} for IgG and 100 pg mL^{-1} for IL-5, using TMB as the enzyme substrate. Most of the reported microfluidic devices did not integrate on-chip raw sample processing. Park *et al.*[105] showed lab-on-a-disc for fully integrated multiplexed immunoassay from raw samples such as whole blood and whole saliva. Biomarkers for cardiovascular disease were detected in this centrifugal PMMA microfluidic layout. Reaction chambers were initially interconnected for sample injection, incubation and washing after which they were isolated for substrate incubation and detection. TMB was used as a substrate for a HRP-conjugated antibody and detected by using the built-in LED and the photodiode. The LOD was found to be 0.30, 0.51, and 0.24 ng mL^{-1} for high-sensitive C-reactive protein (hsCRP), cardiac troponin I (cTnI), and N-terminal pro-B type natriuretic peptide (NT-proBNP), respectively. Additionally, Fang *et al.*[106] showed that loop mediated isothermal amplification (LAMP) of nucleic acid of pseudorabies virus (PRV) integrated in an eight-channel PDMS microfluidic chip. Results could be viewed by the naked eye for insoluble pyrophosphate, a byproduct, or by absorbance, which was measured by optical sensors (high-intensity red light-emitting diode (LED) light at 640 nm and a phototransistor). The assay, which could be completed within an hour, had the LOD of 10 fg μL^{-1} of DNA samples.

Colorimetric results can either be observed with the naked eye or analyzed by software installed on a desktop computer or by applications on mobile phones. For instance, Wang *et al.*[107] developed a tree-shaped paper strip for semi-quantitative colorimetric detection of protein with self-calibration. The approach was validated with bovine serum albumin (BSA) in artificial urine samples with colorimetric detection. They tested a range from 0 to 5 mg mL^{-1} and the concentration as low as 0.08 mg mL^{-1} could be detected using bromophenol blue (BPB) as the indicator. Results were analyzed either by comparison of the color with the naked eye or by measuring the intensities in the standard curve from the software Quantity One. Recently, Ahmed *et al.*[108] demonstrated the power-free enzyme immunoassay for detection of prostate specific antigen (PSA), a biomarker for prostate cancer. Magnetic nanoparticles capture the target and move through chambers having reagents for ELISA. The colour change of a HRP-substrate [ABTS (2,2′-azinobis[3-ethylbenzothiazoline-6-sulfonic acid]-diammonium salt)] in the PMMA based device could be imaged through a smartphone camera and analyzed using Matlab®. The LOD for PSA in serum samples was found to be 3.2 ng mL^{-1}.

Multiple indicators have also been used for multiplexed assay. For example, Dungchai *et al.*[109] reported the use of multiple indicators on μPAD. The oxidation of indicators by hydrogen peroxide produced by oxidase enzymes specific for each analyte gives an extended range of operation. To show the effectiveness of the approach, the mixture of 4-aminoantipyrine and 3,5-dichloro-2-hydroxy-benzenesulfonic acid, *o*-dianisidine dihydrochloride, potassium iodide, acid black, and acid yellow were chosen as the indicators for the simultaneous semi-quantitative measurement of glucose, lactate, and uric acid on a μPAD. They quantified glucose (0.5–20 mM), lactate (1–25 mM), and uric acid (0.1–7 mM) in clinically relevant ranges. The determination of glucose, lactate, and uric acid in control serum and urine samples was performed to demonstrate the applicability of this device for biological sample analysis. Jokerst *et al.*[38] developed a paper-based analytical device for detection of food borne pathogens. Detection was achieved by measuring the color change when an enzyme associated with a pathogen of interest reacts with a chromogenic sub-

strate (β-galactosidase with chlorophenol red β-galactopyranoside (CPRG) for *Escherichia coli*; phosphatidylinositol specific phospholipase C (PI-PLC) with 5-bromo-4-chloro-3-indolyl-myo-inositol phosphate (X-InP) for *Listeria monocytogenes*; and esterase with 5-bromo-6-chloro-3-indolyl caprylate (magenta caprylate) for *Salmonella enterica*). The concentration of 10 cfu cm^{-2} of the target bacterial species was detected within 8, 10, and 12 h of enrichment for *S. typhimurium*, *E. coli* O157:H7, and *L. monocytogenes*, respectively.

Different kinds of nanoparticles have been used in colorimetric detection to increase the sensitivity of the assay. Good optical properties, controlled synthesis and easy surface conjugation make AuNPs one of the most attractive materials for biosensing. Lei *et al.*[110] developed a colorimetric immunoassay chip based on gold nanoparticles (AuNPs) and gold enhancement for amplifying the specific binding signal. The antibody–biotin conjugate were directly immobilized on a 3-aminopropyltriethoxysilane (APTES)–glutaraldehyde modified glass surface. AuNPs were bound to antibodies through biotin–streptavidin linkage. In the gold enhancement process, gold ions in a solution were catalytically deposited onto the AuNPs and aggregated to metallic gold precipitations. The color intensity was mapped to the concentration of immobilized antigen (IgG) in a dynamic range of 1–5000 ng mL^{-1}. Liang *et al.*[111] developed a paper-based microfluidic colorimetric immunodevice based on the Pd/Fe_3O_4@C NPs and flower-like AuNPs for multiplexed colorimetric immunodetection. In the sandwich-type immunodevice, AuNPs were used to immobilize primary antibodies on paper sensing zones, while Pd/Fe_3O_4@C NP-labelled secondary antibodies were employed as the effective peroxidase mimetics to catalyse the chromogenic reactions (TMB and *o*-phenylenediamine as chromogenic substrates). The microfluidic immunodevice showed good colorimetric response to multiple cancer biomarkers with low limits of detection of 1.7 pg mL^{-1} for carcinoembryonic antigen (CEA) and α-fetoprotein (α-AFP). Ornatska *et al.*[54] used redox nanoparticles of cerium oxide as the chromogenic indicator for the colorimetric detection of glucose. Filter paper was first silanized with aminopropyltrimethoxysilane (APTMS), before cerium oxide nanoparticles and glucose oxidase were co-immobilized. In the presence of glucose, the enzymatically-generated hydrogen peroxide induced a colorimetric change of nanoparticles from white-yellowish to dark orange (Fig. 3A).[54] This method involves two enzymatic reactions. In the first step H_2O_2 is released when the oxidase enzyme oxidizes the substrate. In the second step, H_2O_2 is coupled with HRP and the ceria nanoparticles to generate a color change. Hydroxylated Ce^{4+} forms a reddish-orange complex with H_2O_2 with maximum absorbance at 465 nm. They also demonstrated the detection of glucose in human serum samples. The LOD of 0.5 mM glucose and the linear range from 2.5–100 mM were achieved using the colorimetric detection. The bioassay platform could be stored for at least 79 days at room temperature and be reused for 10 consecutive measurement cycles with the same analytical performance. Kumar *et al.*[112] developed a paper-based microfluidic colorimetric device for the detection

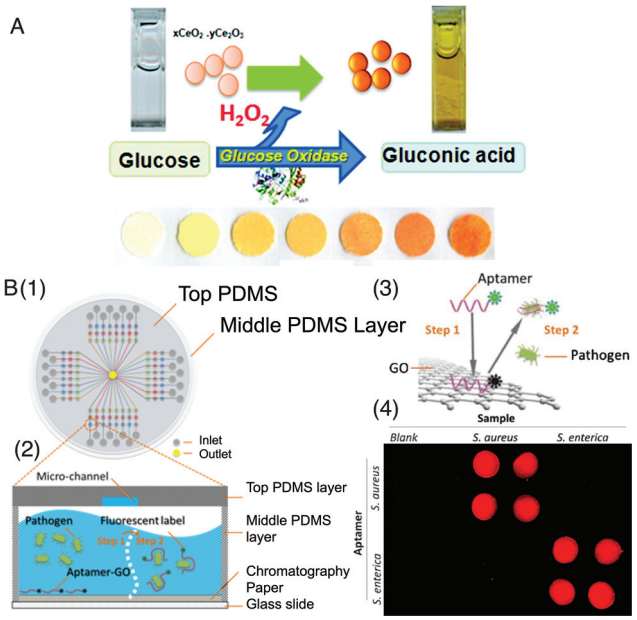

Fig. 3 Biomarker detection using integrated nano-sensors on the chip. (A) Schematic of the working principle of the colorimetric assays for detection of glucose with cerium oxide nanoparticles using a paper-based microfluidic device. Reproduced with permission from American Chemical Society.[54] (B) Schematic of a PDMS/paper hybrid chip for multiplexed one-step pathogen detection using graphene oxide (GO) nanosensors. (1) The hybrid microfluidic biochip layout. (2) and (3) One step turn-on detection based on interaction among GO, aptamers and pathogens. (4) Cross-reaction investigation of *Staphylococcus aureus* and *Salmonella enterica* with their corresponding and non-corresponding aptamers. Reproduced with permission Royal Society of Chemistry.[95]

of uric acid that is associated with several diseases such as diabetes, kidney disease and heart disease. In this microfluidic device, positively charged AuNPs embedded in the device were employed to facilitate the reaction between TMB and H_2O_2 to produce a clear colour change. It was found that the colorimetric method could detect uric acid at a concentration as low as 8.1 ppm. Baeissa *et al.*[113] showed DNA-functionalized monolithic hydrogels and AuNPs for colorimetric DNA detection. Acrydite-modified DNA was covalently functionalized to the polyacrylamide hydrogel during gel formation. By using the attached AuNPs to catalyze the reduction of Ag^+, concentration as low as 1 pM target DNA could be detected. In addition, Wang *et al.*[114] fabricated an integrated microfluidic device using vancomycin-conjugated magnetic beads to capture multiple strains of bacteria and nanogold-labelled specific nucleotide probes for colorimetric PCR-free pathogen detection. The microfluidic device had suction-type micropumps, microvalves, microchannels, and microchambers for complete automation. The LOD of the PDMS microdevice was found to be 10^2 cfu mL^{-1} of *E. coli*.

3.2 Fluorescence detection

The availability of highly sensitive and selective fluorescent labeling techniques makes fluorescence one of the most

widely used optical methods for biomolecular sensing in microfluidic systems. A fluorescent dye, is a small molecule, protein or a quantum dot, which emits a photon after being excited and can be used to label proteins, nucleic acids, or lipids. The detection requires excitation light, fluorescent dyes (if no intrinsic fluorescence), multiple filters, and a detector to record the emitted photons. Compared to colorimetric detection, one of the drawbacks of fluorescence detection is that a fluorescence optical detection system is fairly complex and bulky.

Detection of protein biomarkers for infectious diseases and cancer are some of the different application areas where fluorescence detection has been utilized. Lee *et al.*[42] reported a PDMS microfluidic system utilizing virus-bound magnetic bead complexes for the detection of infections by the dengue virus by the simultaneous rapid detection of immunoglobulin G (IgG) and immunoglobulin M (IgM). IgG and IgM in serum samples were captured by virus-bound magnetic beads.[42] The interfering substances in the biological substances were washed away, after which the fluorescence-labeled secondary antibodies were bound to the surface of the IgG/IgM complex attached onto the magnetic beads. The target IgM and IgG were recognized by the specific attached antibodies (anti-human IgG antibody labeled with fluorescein isothiocyanate (FITC) and anti-human IgM antibody labeled with R-phycoerythrin (R-PE)). The optical signals were then measured and analyzed by a real-time optical detection module. The LOD for IgG was shown to be 21 pg mL^{-1}. Mohammed *et al.*[50] demonstrated a PMMA based autonomous capillary microfluidic system with embedded optics for detection of cTnI, a cardiac biomarker. They used CO_2 laser engraving for rapid prototyping of the capillary system with on-chip planar lenses and bio-sensing elements. The fluoro-immunoassay was done in modified PMMA using FITC. The fluorescence excitation and detection instrumentation was simple, which was palm-sized and battery powered. The LOD was found to be 24 pg mL^{-1}. Diercks *et al.*[115] developed a PDMS microfluidic device for multiplexed protein detection in a nano-liter volume. The chip had optically encoded microspheres to create an array of approximately 100 μm^2 sensors functionalized with capture antibodies directed against distinct targets. The sensitivity of the device was sufficient to detect 1000 copies of the tumor necrosis factor (TNF) in a volume of 4.7 nL. Castro-López *et al.*[116] developed a portable device for the quantification of TNF-α in human plasma with fluorescence detection using the dye fluorescein amidite (FAM). They performed the magnetic bead-based proximity ligation assay (PLA) where probes were immobilized onto streptavidin-coated magnetic beads. The cyclo-olefin polymer based device interfaced with a quantitative real-time PCR device developed in-house, had an assay time of 3 h with the LOD of 3.1 pg mL^{-1}.

Hybrid microfluidic devices that can draw benefits from multiple device substrates have also been developed for the detection of pathogens. Li and his co-workers[95] developed the first PDMS/paper hybrid microfluidic biochip for one-step multiplexed pathogen detection with aptamer-functionalized graphene oxide nano-biosensors (see Fig. 3B). When the Cy3-labeled fluorescent aptamer is adsorbed on the surface of chromatography paper disks inside PDMS microwells, the fluorescence is quenched by graphene oxide (GO) (Fig. 3B(3)).[95] The target pathogen induces the aptamer to be released from GO and thereby restores its fluorescence for detection. The novel use of paper in this hybrid systems facilitated facile nanosensor immobilization on the chip, which avoided complicated surface modification to immobilize nanosensor in non-hybrid microfluidic platforms. The PDMS/paper hybrid microfluidic platform was used for the detection of *Lactobacillus acidophilus* with the LOD of 11.0 colony forming unit (cfu) per mL. The hybrid microfluidic biochip was further used for the simultaneous detection of two infectious pathogens, *S. aureus* and *S. enterica* with high specificity (Fig. 3B(4)). Recently, Dou *et al.*[41] reported a PDMS/paper hybrid microfluidic platform integrated with LAMP for instrument-free infectious disease diagnosis with high sensitivity. As shown in Fig. 2B, the chip consists of a top PDMS layer, a middle PDMS layer, and a glass slide for reagent delivery, LAMP reaction, and structure support, respectively. A chromatography paper disk was placed inside each LAMP zone for preloading LAMP primers. It was found that the use of paper in this hybrid system enabled a longer shelf life time of the hybrid microfluidic platform than a paper-free platform. When a positive sample is shined by a potable UV light pen, bright green fluorescence from calcein can be observed with the naked eye, or imaged by a cell phone camera. The limit of detection of *N. meningitidis* was found to be 3 copies per LAMP zone within 45 min, comparable with that of real-time PCR.[117] This kind of hybrid microfluidic devices can draw more benefits from both substrates, and avoid limitations from individual chip substrates. Jing *et al.*[118] developed a PMMA/PDMS hybrid microfluidic device for efficient airborne bacteria capture and enrichment. The device had two PDMS plates sandwiched by two plates of PMMA using four screws for structural support. Chaotic vortex flow created in the PDMS channel by the staggered herringbone mixer (SHM) resulted in high capture and enrichment as confirmed by flow dynamic mimicking. They showed that the efficiency reached close to 100% in 9 min. The device was validated using *E. coli* and *Mycobacterium smegmatis*. Bacterial cells were quantified with green fluorescence, when exposed to blue light. In addition, Wang *et al.*[61] developed a portable PMMA/glass hybrid microfluidic immunochip for detecting *E. coli* in produce and milk. The PMMA and glass plates were assembled with a double-sided adhesive tape and the microchannels were functionalized using Protein G and NeutrAvidin based methods. Captured bacteria were imaged using an inverted fluorescence microscope through a GFP fluorescence filter. The LOD was found to be 50, 50, 50, and 500 cfus per mL for PBS, blood, milk, and spinach, respectively.

Microfluidic droplets can act as microfluidic bioreactors for enzymatic amplification that has been used to increase the sensitivity of fluorescence detection. For example, Joensson

et al.[119] described a method for the detection and analysis of low-abundance cell-surface biomarkers using enzymatic amplification inside the microscopic droplets within a microfluidic device. Cells were labeled for cell-surface biomarkers with biotinylated antibodies to bind streptavidin-coupled β-galactosidase. The enzyme labeled cell stream was merged with a fluorogenic substrate (fluorescein-di-β-D-galactopyranoside, FDG) in the device. The fluorescence of individual droplets was quantified using laser-induced fluorescence (500–1500 droplets per second). They demonstrated detection of the low-abundance biomarkers CCR5 (a co-receptor in HIV-1 infection) and CD19 (a B-cell lineage marker) from single human monocytic (U937) cells. Recently, Lin *et al.*[120] demonstrated a bubble-driven mixer that was integrated to a microfluidic device for bead-based ELISA to detect bladder cancer. They used a wooden gas diffuser to generate bubbles less than 0.3 mm. The micromixer reduced the time for incubation from 60 min to 8 min, so that ELISA reaction time was reduced to 30–40 min. A fluorescent dye, FITC–streptavidin complex, was used in this PDMS device, wherein magnetic beads were used to coat the primary antibody. Apolipoprotein A1 (APOA1), a biomarker highly correlated with bladder cancer was detected with the LOD of 9.16 ng mL^{-1}, which was lower than the detection cut-off value of 11.16 ng mL^{-1}.

It has always been a great challenge to capture and analyse a small number of circulating tumor cells (CTCs) from a large pool of cancer samples. Riahi *et al.*[121] developed a cyclic olefin polymer (COP) microfluidic device that uses a size and deformability-based capture system to capture and analyse CTCs of breast cancer. The device selects and segregates the CTCs in their own chamber, thus enabling morphological, immunological and genetic characterization of each CTC at the single cell level. Immunostaining of different breast cancer biomarkers was used to further characterize differential expressions of the captured cells. AlexaFlour 488 conjugated antibodies against either vimentin or E-cadherin were used for staining. Nuclei were counterstained with Hoechst-33342. The efficiency of cell capturing ranged between 75–83% for MCF7, 77–85% for MDA-MB-231 and 78–89% for SKBR3 in a range of cells from 20 to 2000. Their result showed that the microfluidic device captured both epithelial cancer cells such as MCF7 and SKBR3 and epithelial to mesenchymal transition (EMT)-like cells such as MDA-MB-231. Immunostaining of captured cells in microchannel devices helped to identify differential expressions and phenotypes of captured cells using a panel of epithelial and mesenchymal breast cancer biomarkers.

Quantum dots (QDs) have advantages over conventional dye molecules such as tunable fluorescence signatures, narrow emission spectra, brighter emission, and good photostability. Use of QDs as a fluorogenic dye can help increase the sensitivity of the assay. Hu *et al.*[122] developed a PDMS microfluidic protein chip for the multiplexed assay of cancer biomarkers using aqueous-phase-synthesized CdTe/CdS quantum dots (aqQDS) as fluorescence signal amplifiers. Secondary antibodies were conjugated to luminescent CdTe/CdS QDs as the fluorescent probe. They showed that their microfluidic protein chip possessed femtomolar sensitivity for cancer biomarkers and was selective enough to be directly used for detection of two biomarkers in serum. The LODs were estimated to be 250 fM for both carcinoma embryonic antigen (CEA, a biomarker for colorectal carcinoma) and α-fetoprotein (AFP, a biomarker for hepatocellular carcinoma). Similarly, Zhang *et al.*[123] developed a PDMS bead-based microfluidic immunosensor using multienzyme-nanoparticle amplification and quantum dots labels. Microbeads were functionalized with capture antibodies and modified electron rich proteins within microfluidic channels. AuNPs were functionalized with a multi-HRP-antibody for enhanced sensitivity. In addition, streptavidin-labeled quantum dots were bound to the deposited biotin moieties as the signal probe. Dual signal amplification resulted in the LOD of 0.2 fg per chip for AFP. Yu *et al.*[124] developed another PDMS microfluidic chip based on a self-assembled magnetic bead pattern and quantum dots for cancer biomarker detection in serum. High magnetic field gradient was generated using the nickel pattern to increase the magnetic force on the superparamagnetic beads (SPMBs), which was stable during fast continuous washing. Fast continuous washing could remove non-specifically adsorptive contaminants more efficiently than fixed volume batch washing, increasing the specificity. Streptavidin modified QDs were used as the fluorescence indicator to obtain the LOD of 3.5 ng mL^{-1} and 3.9 ng mL^{-1} for CEA and AFP, respectively.

Upstream sample processing is often a limiting step in the microfluidic devices. Hoffman *et al.*[125] demonstrated a microfluidic immunoassay with biomarker purification and enrichment. They used stimuli-responsive polymer–antibody conjugates for sample processing in the circular microreactor with transverse flow generators to purify and concentrate the PSA sandwich immunocomplexes. Poly(*N*-isopropylacrylamide) (PNIPAAm), a thermally responsive polymer was covalently grafted to the lysine residues of the anti-prostate specific antigen (an Immunoglobulin G). The antibody–PNIPAAm conjugate and antibody–alkaline phosphatase conjugate formed sandwich immunocomplex *via* PSA binding. Samples were loaded into the device and heated to 39 °C above which the immunocomplexes separate from human plasma solution by immobilizing through hydrophobic interactions. 4-Methylumbelliferyl phosphate (4-MUP) was used as the fluorescence substrate for the alkaline phosphatase conjugated antibody in the PDMS device. For subsequent separation, enrichment, and quantification, these complexes were loaded into a recirculating PDMS bioreactor, which was equipped with micropumps, and transverse flow features. In order to enrich immunocomplexes within the recirculator, the loading, washing, and mixing steps were repeated for a total of three times. The assay which took 25 min had the LOD of 37 pM PSA. By repeating the capture process for three times for immunocomplex enrichment, the LOD of 0.5 pM was obtained. As shown in Table 1, this is much lower than the LOD from colorimetric detection.[108]

3.3 Electrochemical detection

Electrochemical detection involves interaction of chemical species with electrodes or probes to obtain electrical signals, such as potential or current, enabling quantitative analysis of target analytes. Either a chemical reaction is promoted by passing an electrical current through the electrode system or electrode responses are triggered due to specific chemical reactions (oxidation and reduction). A typical electrolytic cell consists of a working electrode where detection of a certain analyte is analyzed, a reference electrode where a standard oxidation/reduction is conducted and a counter electrode to minimize the electrical current flowing through the reference electrode, thus maintaining its potential constant during the operation of the electrolytic cell. Recently, incorporation of electrochemical detection in paper-based microfluidic devices has led to the development of easy-to-use, low cost, portable diagnostic devices with high sensitivity and selectivity by suitable choices of detection potential and/or electrode materials, as shown by many reports of paper-based electrochemical systems listed in Table 1. Microfluidic channels can be fabricated on cellulose paper using different techniques mentioned before, while electrodes can be fabricated on paper by methods including screen-printing, direct-writing with a pen/pencil dispensing conductive material, physical deposition of metals, and spraying conductive inks through stencils.[126] However, screen-printing approach remains the most common technique for electrode fabrication.[127]

In recent years, great efforts have been devoted for the development of electrochemical detection-based microfluidic devices for disease diagnosis especially for the detection of cancer biomarkers and infectious diseases.[128,129] Li *et al.*[130] described an electrochemical ELISA on paper-based microfluidic devices. Paper-based microfluidic devices were fabricated by patterning chromatography paper using the photolithography technique. Working and counter electrodes were screen-printed from graphite ink, and a reference electrode from silver/silver chloride ink. The electrochemical ELISA of IgG based on cyclic voltammetry (CV) was demonstrated with the LOD of 3.9 fM. Wu *et al.*[31] developed a microfluidic paper-based electrochemical immunodevice integrated with amplification-by-polymerization for multiplexed detection of cancer biomarkers by using the differential pulse voltammetry (DPV) method. In this work, the paper-based immunodevice was prepared based on the photoresist-patterning technique (Fig. 4).[31] Eight working electrode zones were screen-printed with carbon ink in a specific area on paper-A. In the same manner, carbon ink and Ag/AgCl ink were screen-printed on a predesigned area of paper-B as the counter electrode and the reference electrode, respectively. Eight working electrodes shared one pair of counter and reference electrodes after the two paper layers were stacked together (Fig. 4A). GO was modified on the working electrode to construct the sandwiched immuno-structure (Fig. 4B). Four cancer biomarkers, namely carcinoembryonic antigen (CEA), AFP, cancer antigen 125 (CA-125, a biomarker for ovarian cancer), and carbohydrate antigen 153 (CA153, a biomarker for breast cancer) were detected by using the HRP–*O*-phenylenediamine–H_2O_2 electrochemical system. The LODs were found to be 0.01 ng mL^{-1}, 0.01 ng mL^{-1}, 0.05 ng mL^{-1}, and 0.05 ng mL^{-1}, respectively. Chikkaveeraiah *et al.*[49] reported a microfluidic electrochemical immunoassay for multiplexed detection of cancer biomarkers using a molded PDMS channel and routine machined parts interfaced with a pump and sample injector. The LODs of 0.23 pg mL^{-1} for PSA and 0.30 pg mL^{-1} for interleukin 6 (IL-6) were obtained in diluted serum mixtures. In addition, Su *et al.*[55] developed a paper-based microfluidic electrochemical cytodevice (μ-PECD) for cancer cell detection and *in situ* screening of anticancer drugs in a multiplex manner based on in-electrode 3D cell culture. This entire μ-PECD was fabricated on a single sheet of flat paper. The LOD for the HL-60 (human acute promyelocytic leukemia) cell was calculated to be 350 cells per mL using the fast-response DPV method. Furthermore, *in situ* anticancer drug screening was successfully implemented in this μ-PECD. Sun *et al.*[131] presented a paper-based microfluidic electrochemical immunosensor for CEA detection based on a 3D flower-like gold electrode and gold–silver bimetallic nanoparticles. The LOD was found to be 0.3 pg mL^{-1} using an amperometric method.

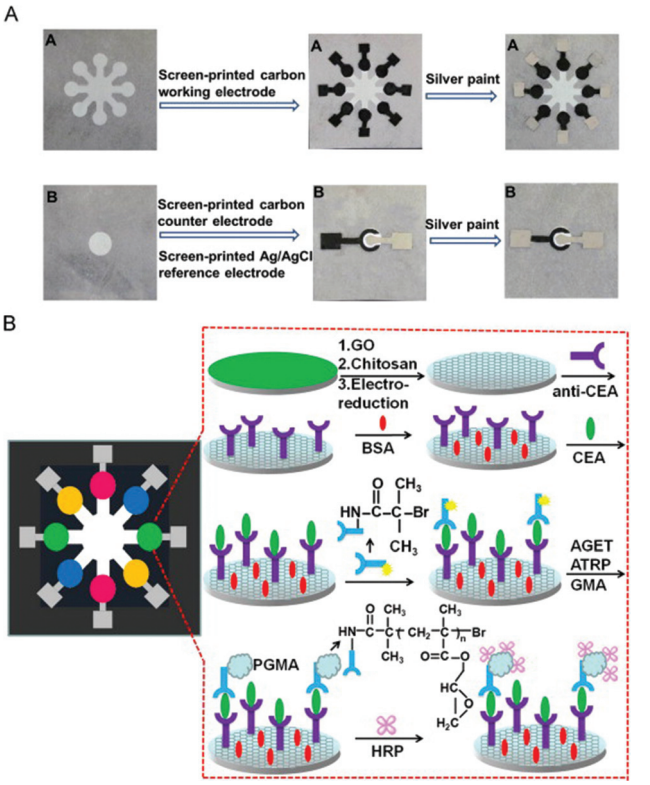

Fig. 4 A paper-based microfluidic platform with electrochemical detection for multiplexed cancer biomarker detection. (A) Device fabrication procedures. (B) Schematic representation of the electrochemical immunoassay procedures using CEA as an example. Reproduced with permission from Elsevier.[31]

The physical adsorption may result in strong non-specific binding.[132] Hence, device surfaces can be modified for the covalent immobilization of antibodies to increase the sensitivity for immunoassay of biomarkers. Wang *et al.*[33] demonstrated an electrochemical immunoassay on a wax-patterned paper-based 3D microfluidic electrochemical device (3D-μPED) using the DPV method. Paper pre-coated with chitosan and cross-linked with glutaraldehyde was used to immobilize antibodies for CA-125 and CEA. The multi-walled carbon nanotube (MWCNT)-modified μPAD could detect two tumor markers simultaneously in real clinical serum samples with linear ranges of 0.001–75.0 U mL^{-1} for CA-125 and 0.05–50.0 ng mL^{-1} for CEA. The LODs for CA-125 and CEA were 0.2 mU mL^{-1} and 0.01 ng mL^{-1}, respectively. Liu *et al.*[133] developed a PMMA microfluidic chip coupled with a three-electrode electrochemical detection system to detect the trace level of AFP. For covalent immobilization of the AFP monoclonal antibody, PMMA microchannels were first modified with poly(ethyleneimine). The captured analyte, AFP, was finally bound to the HRP-conjugated AFP antibody for electrochemical detection. When the substrate mixture of 2-amino hydroxybenzene and hydrogen peroxide was pumped into the PMMA microchannel, the HRP enzyme labeled on the AFP antibody within microchannels would instantaneously catalyze the substrate, and the generated electroactive 3-amino phenoxazine was detected using differential pulse voltammetry (DPV). The immunochip had the LOD of 1 pg mL^{-1} for AFP with a detectable linear concentration range of 1–500 pg mL^{-1}. AFP existing in healthy human serum was detected to demonstrate the application of the immunochip.

Cardiovascular disease is one of the leading causes of death in the world. Multiple microfluidic electrochemical systems were developed to measure heart disease biomarkers. Zhou *et al.*[134] developed an electrochemical immunoassay for the simultaneous detection of cardiac cTnI and the c-reactive protein (CRP) on a PDMS microfluidic chip. Cardiac troponin I is used to diagnose acute myocardial infarction. The CRP is used in the risk assessment of coronary events and in optimizing therapy in the primary and secondary prevention settings of cardiovascular diseases. The methodology was based on ELISA performed in PDMS–gold nanoparticle composite microreactors. The sandwich immunoassay was done by bioconjugating CdTe and ZnSe quantum dots. Cd^{2+} and Zn^{2+} were detected by square-wave anodic stripping voltammetry for quantification of the two biomarkers. The immunosensor could simultaneously detect cTnI and CRP in the linear ranges between 0.01–50 μg L^{-1} and 0.5–200 μg L^{-1} respectively. They showed that the limits of detection were 5 amol and 307 amol in a 30 μL sample corresponding to cTnI and CRP, respectively. Liang *et al.*[135] developed a microfluidic electrochemical immunoassay for the detection of heart failure markers, amino-terminal pro-brain natriuretic peptides (NT-proBNP), in whole blood with the LOD of 0.03 ng mL^{-1}. Magnetic nanoparticles and the biotin–avidin system were employed in the microfluidic device to fabricate the regeneration-free electrochemical immunosensor. Recently, Horak *et al.*[43] presented a polymer-modified microfluidic immunochip for enhanced electrochemical detection of a cardiac biomarker, troponin I. The combination of a disposable microfluidic immunochip fabricated in a Vacrel® 8100 photoresist film and surface functionalization by polyethylenimine (PEI) was used to construct the microfluidic device. An 18-fold improvement of the LOD and 2.5 times faster read-out time in comparison with the assay without the PEI coating were achieved with the LOD of 25 pg mL^{-1}.

Microfluidic electrochemical devices have also been used for the detection of other important biomarkers. Medina-Sánchez *et al.*[45] reported an electrochemical assay for apolipoprotein E (ApoE, a biomarker of Alzheimer's disease) using cadmium-selenide/zinc-sulfide quantum dots as the labeling carrier. The electrochemical detector consisted of a set of three electrodes produced by screen-printing with a micro-potentiostat. A PDMS film was bound to the APTES modified PC substrate after plasma treatment for irreversible bonding. Tosyl activated magnetic beads were used as a pre-concentration platform for the immunoassay. The use of a microchannel with a magnetic retention zone allowed the sample purification and pre-concentration using magnetic beads as stationary support, providing good sensitivity and control. Electrochemical detection was obtained by square wave anodic stripping voltammetry. The limit of detection was found to be 12.5 ng mL^{-1} with a linearity range from 10 to 200 ng mL^{-1}. Zhao *et al.*[136] reported a paper-based microfluidic electrochemical array for multiplexed detection of metabolic biomarkers. An array of eight electrochemical sensors and a handheld custom-made electrochemical reader for signal readout were employed in the device for the simultaneous detection of glucose, lactate and uric acid in urine with the limits of detection of 0.35 mM, 1.76 mM, and 0.52 mM, respectively. Recently, Ben-Yoav *et al.*[137] illustrated a controllable PDMS microfluidic electrochemical method for label-free analysis of DNA hybridization in diagnosis of genetic disorders. The theoretical LOD was found to be 1 nM of complementary ssDNA target using the CV method.

3.4 Chemiluminescence detection

Chemiluminescence (CL) is another optical detection method for analyte detection in which target binding leads to certain chemical reactions to cause photochemical emission, either directly or with the help of an enzyme label. CL detection systems may be more convenient for point-of-care setting, because this technique does not require excitation light source and emission filters as compared to fluorescence detection. However, the development of low-cost photodetectors is still necessary for its wide application in POC settings.[138,139]

Chemiluminescence detection of various cancer biomarkers has been achieved in different microfluidic platforms. Wang *et al.*[32] described a paper-based microfluidic chemiluminescence ELISA. The μPAD was fabricated by the wax-screen printing method and modified with chitosan. Luminol–*p*-iodophenol–H_2O_2 solution was used as the substrate for HRP-CL. Chemiluminescence ELISA showed the linear ranges

of 0.1–35.0 ng mL^{-1} for AFP, 0.5–80.0 U mL^{-1} for CA-125 and 0.1–70.0 ng mL^{-1} for CEA. The LODs were found to be 0.06 ng mL^{-1}, 0.33 ng mL^{-1}, and 0.05 ng mL^{-1} for AFP, CA-125, and CEA, respectively. Ge *et al.*[140] developed a 3D origami paper-based analytical device for the multiplexed chemiluminescence immunoassay. Blood plasma separation from whole blood and rinse steps were integrated into the device. Ag nanoparticles were used to catalyze a typical luminol–H_2O_2 CL system. The LODs for simultaneous detection of four tumor biomarkers AFP, CA 153, CA 199, and CEA were found to be 1 ng mL^{-1}, 0.4 U mL^{-1}, 0.06 U mL^{-1}, and 0.02 ng mL^{-1}, respectively. In addition, chemiluminescence has also been used to study the human thyroid stimulating hormone. Matos Pires *et al.*[141] developed an HRP–luminol–peroxide-based chemiluminescence biosensor using an integrated polycarbazole photodiode as the detector. A chemiluminescence immunoassay was performed in a PDMS–gold–glass microfluidic chip. The human thyroid stimulating hormone was detected with a linear range from 0.03 to 10 ng mL^{-1} and the LOD was found to be 68 pg mL^{-1}.

AuNPs were used in microfluidic CL detection to enhance the detection sensitivity. For instance, Liu *et al.*[142] showed chemiluminescence detection of rare cells based on aptamer-specific capture in PDMS microfluidic channels. Biotinylated aptamers were immobilized in the channel by the strong adsorption of avidin to the glass surface and then the avidin–biotin system (Fig. 5A).[142] Specific cells (CCRF-CEM cell line (CCL-119, T cell line, human acute lymphoblastic leukemia) and Ramos cell line (CRL-1596, B cell line, human Burkitt's lymphoma)) from a cell mixture were captured and isolated by aptamers immobilized in the microfluidic channel. CL reaction was then triggered by the addition of AuNPs modified with aptamers to bind to the cells. Based on the luminol–H_2O_2–AuNPs CL reaction, the CL signal could be detected when a luminol–H_2O_2 solution was pumped into the microfluidic channel. A PMT was placed directly underneath the PDMS microfluidic channel for CL detection. A low LOD of 30 target cells in a 3 μL cell mixture was obtained. Spiked whole blood samples were also used to verify the practicality of the method for inexpensive and rapid CL detection. Yang *et al.*[143] described a gold nanoparticle enhanced chemiluminescence immunosensor for the detection of Staphylococcal Enterotoxin B (SEB), which is a major cause of foodborne diseases. The anti-SEB antibody–gold nanoparticle complex was immobilized on a polycarbonate surface and detected by a sandwich immunoassay. The signal was detected by using a portable detector based on a cooled CCD sensor or a plate reader, and the LOD was found to be 0.01 ng mL^{-1}.

Microfluidic microarrays have also been used for high-throughput chemiluminescence detection. Zhao *et al.*[144] developed a low-cost 1536 chamber microfluidic microarray for mood-disorder-related serological studies. In the pilot study they quantified 384 serological biomarkers. The device was modeled similar to 1536-well microtiter plate for measuring chemiluminescence immunoassay (SuperSignal® as a substrate) using a microplate reader. The modified PMMA platform showed a similar LOD as standard ELISA but with reduced operation time (1/2 h). Matos Pires *et al.*[51] developed a PMMA microfluidic biosensor array for multiplexed detection of pathogens. Organic blend heterojunction photodiodes were integrated for chemiluminescence. *E. coli*, *Campylobacter jejuni* and adenovirus were targeted in the PMMA chip, and detection of captured pathogens was conducted by using poly(2,7-carbazole)/fullerene organic photodiodes (OPDs). Chemiluminescence signal was obtained from SuperSignal® chemiluminescence reagents added onto the streptavidin–HRP conjugate. The LOD was found to be 5×10^5 cells per mL for *E. coli*, 1×10^5 cells per mL for *C. jejuni*, and 1×10^{-8} mg mL^{-1} for adenovirus.

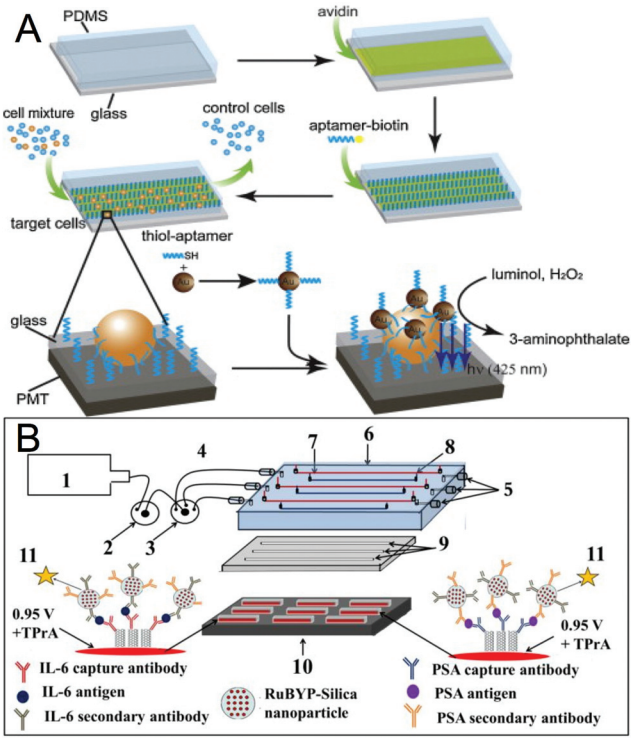

Fig. 5 Biomarker detection on microfluidic platforms with chemiluminescence and electrochemiluminescence detection. (A) Schematic representation of rare cell capture and detection using aptamers and chemiluminescence. Reproduced with permission from Elsevier.[142] (B) Microfluidic electrochemiluminescence array for cancer biomarker detection. (1) Syringe pump; (2) injector valve; (3) switch valve; (4) tubing for inlet; (5) outlet; (6) PMMA plate; (7) Pt counter wire; (8) Ag/AgCl reference wire; (9) PDMS channels; (10) pyrolytic graphite chip; (11) immunoassay complex on RuBPY–silica nanoparticles. Reproduced with permission from Springer.[36]

3.5 Electrochemiluminescence detection

ECL detection combines electrochemical and luminescence techniques that can provide good selectivity and sensitivity wherein a set of electrodes is used to trigger and control a chemiluminescence reaction involving an ECL active luminophore compound.[145] ECL has been widely applied in microfluidic analytical methods for biomarker detection for disease diagno-

sis due to its unique advantages. The outstanding advantage is its versatility and simplified optical setup compared to photoluminescence, and good temporal and spatial control compared to chemiluminescence. It does not require a bulky light source like fluorescence detection and can be generated on an electrode or a chip. Additionally, the background signal is negligible, thereby allowing optical detectors to be used at their maximum sensitivity. As summarized in Table 1, interest in paper-based ECL sensors has been shown recently.

Among various applications of microfluidic ECL biomarker detection,[146] the detection of cancer biomarkers for cancer diagnosis has been the subject of great research interest, as shown in Table 1. Ge *et al.*[147] reported a 3D microfluidic paper-based ECL immunodevice for multiplexed measurement of tumor biomarkers. In this work, a wax-patterned paper-based device using the typical tris-(bipyridine)–ruthenium(II)–tri-*n*-propylamine ECL system was reported. The LODs were found to be 0.15 ng mL^{-1}, 0.6 U mL^{-1}, 0.17 U mL^{-1}, and 0.5 ng mL^{-1} for AFP, CA-125, CA-199, and CEA, respectively. Yang *et al.*[148] fabricated a paper-based microfluidic pen-on-paper ECL (PoP-ECL) immunodevice for POC determination of CA-199 with the LOD of 0.0055 U mL^{-1}. The PoP-ECL device was constructed with a hydrophilic paper channel and two PoP electrodes with a rechargeable battery as the constant-potential power supplier to trigger the ECL. Sardesai *et al.*[36] described a PMMA/PDMS microfluidic ECL device for detecting cancer biomarker proteins, PSA and IL-6 in serum (Fig. 5B).[36] The microfluidic system employed three PDMS channels on a conductive pyrolytic graphite chip (2.5 × 2.5 cm) inserted into a machined chamber and interfaced with a pump, switching valve, and sample injector. The antigens were captured by capture-antibody decorated single-walled carbon nanotubes (SWCNT) fabricated at the bottom of the wells. Then, a RuBPY–silica–secondary antibody (Ab2) label was injected to bind to the antigen on the array, followed by injection of sacrificial reductant tripropylamine (TPrA) to produce ECL. Potential applied *versus* Ag/AgCl oxidized TPrA to produce ECL by redox cycling the RuBPY species on the particles, which was measured by a CCD camera. The microfluidic ECL array provided sensitivity at clinically relevant levels of PSA from 100 fg mL^{-1} to 10 ng mL^{-1} and IL-6 from 10 fg mL^{-1} to 1 ng mL^{-1}. The LODs were found to be 100 fg mL^{-1} (9 zeptomole) for PSA and 10 fg mL^{-1} (1 zeptomole) for IL-6. The assay of synthetic human serum samples in the microfluidic array was compared with single protein ELISAs, and *t* tests at 95% confidence level confirmed that there was no significant difference between the two methods. Additionally, Li *et al.*[34] demonstrated a battery-triggered ECL paper-based immunodevice for a multiplexed immunoassay. They used dual-signal amplification strategy by using a GO-chitosan/gold nanoparticles (GCA) immunosensing platform and a [4,4-(2,5-dimethoxy-1,4-phenylene)bis(ethyne-2,1-diyl)dibenzoic acid] (P-acid) functionalized nanoporous silver (P-acid/NPS) signal amplification label. The corresponding capture antibodies were immobilized onto paper working zones on the back of screen-printed carbon working electrodes. PSA and CEA were detected in the linear ranges of 0.003–20 ng mL^{-1} and 0.001–10 ng mL^{-1} with the LODs down to 1.0 pg mL^{-1} and 0.8 pg mL^{-1}, respectively.

Different nanomaterials such as AuNPs and graphene have been employed for microfluidic ECL biomarker detection. Wu *et al.*[30] developed a paper-based microfluidic electrochemiluminescence origami cyto-device (μ-PECLOC) with aptamer-modified Au electrodes. Wax-fabricated paper was used for screen-printing of the electrode array. Paper was modified through growth of the layer of Au nanoparticles on the surfaces of cellulose fibers to form a 3D macroporous Au-paper cell electrode (PCE) array for the immobilization of aptamers. Owing to the effective disproportionation of hydrogen peroxide and specific recognition of mannose on the cell surface, concanavalin-A conjugated porous AuPd alloy nanoparticles were introduced into this μ-PECLOC as the catalytically promoted nanolabels for the peroxydisulfate ECL system. The ECL intensity was found to be logarithmically related to the concentration of MCF-7 cells in the range of 450–1.0 × 10^7 cells per mL with the LOD of 250 cells per mL. To further improve the detection performance, nanomaterials with good sensing properties have been incorporated into the microfluidic ECL device. Wang *et al.*[35] developed a paper-based 3D microfluidic ECL immunosensor for POC detection of CA-125. To construct a sensitivity-enhanced sandwich-type ECL immunosensor in the microfluidic device, AuNPs were employed as both the pathway of electron transfer and the probe to label the signal antibody. AuNPs can overcome the poor sensitivity, poor stability, and safety problems associated with the use of radioisotopic, fluorescent, and enzyme label.[149] The device had the LOD of 0.0074 U mL^{-1} for CA-125. Xu *et al.*[150] established a paper-based solid-state ECL sensor using a poly(sodium 4-styrenesulfonate) functionalized graphene/nafion composite film for discrimination of single-nucleotide mismatch in human urine matrix. Li *et al.*[151] developed a microfluidic paper-based ECL sensor for DNA detection using a graphene-modified Au-paper working electrode and calcium carbonate/carboxymethyl chitosan hybrid microspheres on luminescent silver nanoparticle (AgNP) composites. The paper-based DNA sensor could detect target DNA in the range of 4.0 × 10^{-17}–5.0 × 10^{-11} M, with the LOD of 8.5 × 10^{-18} M.

3.6 Other detection methods

Several other detection mechanisms have been utilized on the microfluidic devices. Koh *et al.*[152] developed bead affinity chromatography (BAC) in a temperature controlled PDMS microsystem for detection of biomarkers and preparation of samples for matrix assisted laser desorption/ionization time of flight mass spectrometry (MALDI-TOF MS) analysis. RNA aptamer-immobilized microbeads capture cancer biomarkers in BAC, which can be denatured and released by controlling the temperature. CEA was concentrated and purified from human serum in the microsystem and detected by MALDI-TOF MS. Mousavi *et al.*[153] used capped gold nanoslit surface plasmon resonance (SPR) on a PMMA microfluidic chip for detection of a urinary micro-RNA biomarker. They used magnetic nanoparticles for the isolation of the target molecule and

enhancement of signal in conjunction with SPR on capped gold nanoslit. miRNA-16-5p, a specific and noninvasive biomarker for acute kidney injury (AKI) was detected with a LOD of 17 fM. Zhou *et al.*[37] described localized surface plasmon resonance (LSPR) on a glass/poly(olygo(ethylene glycol) methacrylate) (POEGMA) microfluidic device. The fluorescent dyes conjugated to the analyte were excited by plasmonic field to increase the sensitivity. The chip was inserted into a POC system, which had micropumps to control the microfluidic flow, a light source for fluorescence excitation, a camera system for fluorescence detection, and software to automate the POC system and to analyze the result. The LOD for PSA was found to be 100 pg mL^{-1}. Tian *et al.*[154] developed a different LSPR-based microfluidic device using antibody-functionalized gold nanorods on common laboratory filter paper to produce a bioplasmonic nanostructure for sensitive detection of bioanalytes in physiological fluids. Zhang *et al.*[48] developed a PDMS microfluidic device for automatic detection of CEA in exhaled breath condensate (EBC) using a long wave surface acoustic wave (SAW) immunosensor. A sandwich immunoassay using antibody labeled with AuNPs and subsequently mass enhancement using gold staining solutions showed good sensitivity with the LOD of 1.25 ng mL^{-1}. Due to multiple advantages of bioplasmonic paper such as high specific surface area, mechanical flexibility, compatibility with conventional printing approaches, it was used for rapid and label-free detection of proteins such as aquaporin-1 (AQP1), a biomarker for the early detection of renal cancer carcinoma (RCC), with the LOD of about 24 pg mL^{-1} in artificial urine.

4 Conclusions and future prospects

A number of microfluidic platforms including different polymers, paper-based, and hybrid microdevices have been developed for rapid detection of biomarkers of infectious diseases, cancer and other diseases (Table 1). Microfluidic platforms offer many advantages over conventional diagnosis methods, such as low cost, ease of use, high portability or disposability. With the progress in fabrication technology, it is now possible to tailor a fabrication material ranging from polymers to paper and devise a method to match the cost and application of the device. It has been demonstrated that these microfluidic devices have emerged as promising diagnostic platforms to improve human health in low resource settings.

Despite the exciting progress in the field, there are still many hurdles for the application of microfluidic biochips as routine diagnostic devices, especially for field diagnosis and POC diagnosis in low-resource settings. For example, many microfluidic devices still use complex detection methods and require expensive external equipment, which limits the use of these devices as POC detection in low-resource settings. Although colorimetric detection is highly simple and suitable for low-resource settings, sensitivity and quantitation are often compromised. Electrochemical detection is highly sensitive and quantitative, but smaller and inexpensive electrochemical analyzers are expected to offer advantage in electrochemical detection for the field diagnosis. Optical detection remains an attractive technique for microfluidic analysis of pathogens and proteins, although integrating sensitive optical detectors in inexpensive microfluidic-based devices remains a bottleneck to develop POC devices. An increasing number of new Apps and add-ons have enabled powerful smartphones to perform more and more functions for monitoring personal health status.[155] There have been reports of full laboratory-quality immunoassay that can be run on a smartphone accessory.[156] Therefore, we believe that the combination of smartphone technologies with microfluidic devices could cause great impacts on health care (*i.e.* mHealth) and disease monitoring in the near future to make certain laboratory-based diagnostics accessible to people with smartphone access.

The future trend in microfluidic devices also includes new methods for sample collection and preparation, reagent storage and fully integrated lab-on-a-chip. Sample preparation on a chip is often not considered and there are only a small number of devices that offer total analysis on chip.[57,157,158] Microfluidic biochips that can directly test crude real-world samples (*e.g.* blood, urine, and saliva) may be the alternative to sample preparation on a chip. Similarly, validation of the on-chip detection approaches against real samples is a requirement for successful adoption of these systems by the clinical personnel. Although, there are a vast number of reported microfluidic devices for detection of different diseases, commercialization of these devices and their use outside the research laboratories remain a major challenge. It may be because current clinical diagnostic approaches are well developed and accepted over a long period of time. Hence, the microfluidic platforms do need to solve those challenging real-world issues, and demonstrate robustness and convincing advantages of microfluidic biochips over conventional methods to the clinical personnel before they are widely used by them. More exciting work is expected from the close collaboration and exchange between the microfluidic lab-on-a-chip community, and the biological and clinical communities.

Acknowledgements

The Li group would like to acknowledge financial support of the National Institute of Allergy and Infectious Diseases of the National Institutes of Health (NIH) under award number R21AI107415, and the National Institute of General Medical Sciences of the NIH under award number SC2GM105584. The content is solely the responsibility of the authors and does not necessarily represent the official views of the NIH. Financial support from the IDR Program at the University of Texas at El Paso (UTEP) and the NIH RCMI Pilot Grant are also gratefully acknowledged. F.X. would like to acknowledge financial support of the Key (Key grant) Project of Chinese Ministry of Education (313045) and the International Science & Technology Cooperation Program of China (2013DFG02930). We are

also grateful to Mr. Misael Rios for his contribution in preparing figures

Notes and references

1 F. Biomedical, *Clin. Pharmacol. Ther.*, 2001, **69**, 89–95.
2 L.-Y. Hung, H.-W. Wu, K. Hsieh and G.-B. Lee, *Microfluid. Nanofluid.*, 2014, **16**, 941–963.
3 B. Adamczyk, T. Tharmalingam and P. M. Rudd, *Biochim. Biophys. Acta*, 2012, **1820**, 1347–1353.
4 S. B. Baylin and P. A. Jones, *Nat. Rev. Cancer*, 2011, **11**, 726–734.
5 X. Luo and J. J. Davis, *Chem. Soc. Rev.*, 2013, **42**, 5944–5962.
6 R. Lozano, M. Naghavi, K. Foreman, S. Lim, K. Shibuya, V. Aboyans, J. Abraham, T. Adair, R. Aggarwal and S. Y. Ahn, *Lancet*, 2013, **380**, 2095–2128.
7 K. E. Nelson and C. M. Williams, *Infectious disease epidemiology*, Jones & Bartlett Publishers, 2012.
8 P. Yager, G. J. Domingo and J. Gerdes, *Annu. Rev. Biomed. Eng.*, 2008, **10**, 107–144.
9 M. Harris and J. Reza, *Global report for research on infectious diseases of poverty*, World Health Organization, 2012.
10 J. Ferlay, I. Soerjomataram, R. Dikshit, S. Eser, C. Mathers, M. Rebelo, D. M. Parkin, D. Forman and F. Bray, *Int. J. Cancer*, 2015, **136**, E359–E386.
11 J. Ferlay, I. Soerjomataram, R. Dikshit, S. Eser, C. Mathers, M. Rebelo, D. M. Parkin, D. Forman and F. Bray, *Int. J. Cancer*, 2015, **136**, E359–E386.
12 D. Wild, *The Immunoassay Handbook: Theory and applications of ligand binding*, ELISA and related techniques, Newnes, 2013.
13 M. A. Innis, D. H. Gelfand, J. J. Sninsky and T. J. White, *PCR protocols: a guide to methods and applications*, Academic press, 2012.
14 D. L. Jaye, R. A. Bray, H. M. Gebel, W. A. Harris and E. K. Waller, *J. Immunol.*, 2012, **188**, 4715–4719.
15 M. Urdea, L. A. Penny, S. S. Olmsted, M. Y. Giovanni, P. Kaspar, A. Shepherd, P. Wilson, C. A. Dahl, S. Buchsbaum and G. Moeller, *Nature*, 2006, **444**, 73–79.
16 X. Li and P. C. Li, *Expert Rev. Clin. Pharmacol.*, 2010, **3**, 267–280.
17 A. Arora, G. Simone, G. B. Salieb-Beugelaar, J. T. Kim and A. Manz, *Anal. Chem.*, 2010, **82**, 4830–4847.
18 M. L. Kovarik, P. C. Gach, D. M. Ornoff, Y. Wang, J. Balowski, L. Farrag and N. L. Allbritton, *Anal. Chem.*, 2011, **84**, 516–540.
19 J. Hu, S. Wang, L. Wang, F. Li, B. Pingguan-Murphy, T. J. Lu and F. Xu, *Biosens. Bioelectron.*, 2014, **54**, 585–597.
20 S. Wang, F. Xu and U. Demirci, *Biotechnol. Adv.*, 2010, **28**, 770–781.
21 F. Shen, X. Li and P. C. H. Li, *Biomicrofluidics*, 2014, **8**, 014109.
22 X. J. Li and Y. Zhou, *Microfluidic devices for biomedical applications*, Elsevier, 2013.
23 J. Liang, Y. Wang and B. Liu, *RSC Adv.*, 2012, **2**, 3878–3884.
24 H. Qi, G. Huang, Y. L. Han, W. Lin, X. Li, S. Wang, T. J. Lu and F. Xu, *Crit. Rev. Biotechnol.*, 2014, 1–12, July 15.
25 X. Li and P. C. Li, *Can. J. Pure Appl. Sci.*, 2014, **8**, 2663–2669.
26 X. Li, Y. Chen and P. C. Li, *Lab Chip*, 2011, **11**, 1378–1384.
27 X. Li, V. Ling and P. C. Li, *Anal. Chem.*, 2008, **80**, 4095–4102.
28 H. Chen, X. Li, L. Wang and P. C. Li, *Talanta*, 2010, **81**, 1203–1208.
29 X. Li, A. V. Valadez, P. Zuo and Z. Nie, *Bioanalysis*, 2012, **4**, 1509–1525.
30 L. Wu, C. Ma, L. Ge, Q. Kong, M. Yan, S. Ge and J. Yu, *Biosens. Bioelectron.*, 2015, **63**, 450–457.
31 Y. Wu, P. Xue, K. M. Hui and Y. Kang, *Biosens. Bioelectron.*, 2014, **52**, 180–187.
32 S. Wang, L. Ge, X. Song, J. Yu, S. Ge, J. Huang and F. Zeng, *Biosens. Bioelectron.*, 2012, **31**, 212–218.
33 P. Wang, L. Ge, M. Yan, X. Song, S. Ge and J. Yu, *Biosens. Bioelectron.*, 2012, **32**, 238–243.
34 W. Li, M. Li, S. Ge, M. Yan, J. Huang and J. Yu, *Anal. Chem. Acta*, 2013, **767**, 66–74.
35 S. Wang, L. Ge, M. Yan, J. Yu, X. Song, S. Ge and J. Huang, *Sens. Actuators, B*, 2013, **176**, 1–8.
36 N. P. Sardesai, K. Kadimisetty, R. Faria and J. F. Rusling, *Anal. Bioanal. Chem.*, 2013, **405**, 3831–3838.
37 X. D. Zhou, T. I. Wong, H. Y. Song, L. Wu, Y. Wang, P. Bai, D. H. Kim, S. H. Ng, M. S. Tse and W. Knoll, *Plasmonics*, 2014, **9**, 835–844.
38 J. C. Jokerst, J. A. Adkins, B. Bisha, M. M. Mentele, L. D. Goodridge and C. S. Henry, *Anal. Chem.*, 2012, **84**, 2900–2907.
39 L. Yu, C. M. Li, Y. Liu, J. Gao, W. Wang and Y. Gan, *Lab Chip*, 2009, **9**, 1243–1247.
40 M. Dou, D. C. Dominguez, X. Li, J. Sanchez and G. Scott, *Anal. Chem.*, 2014, **86**, 7978–7986.
41 M. Dou, D. C. Dominguez, X. Li, J. Sanchez and G. Scott, *Anal. Chem.*, 2014, **86**, 7978–7986.
42 Y.-F. Lee, K.-Y. Lien, H.-Y. Lei and G.-B. Lee, *Biosens. Bioelectron.*, 2009, **25**, 745–752.
43 J. Horak, C. Dincer, E. Qelibari, H. Bakirci and G. Urban, *Sens. Actuators, B*, 2014, **209**, 478–485.
44 X. J. Li and P. C. H. Li, *Anal. Chem.*, 2005, **77**, 4315–4322.
45 M. Medina-Sánchez, S. Miserere, E. Morales-Narváez and A. Merkoçi, *Biosens. Bioelectron.*, 2014, **54**, 279–284.
46 X. J. Li, X. Xue and P. C. H. Li, *Integr. Biol.*, 2009, **1**, 90–98.
47 X. J. Li, J. Huang, G. F. Tibbits and P. C. H. Li, *Electrophoresis*, 2007, **28**, 4723–4733.
48 X. Zhang, Y. Zou, C. An, K. Ying, X. Chen and P. Wang, *Sens. Actuators, B*, 2014, **205**, 94–101.
49 B. V. Chikkaveeraiah, V. Mani, V. Patel, J. S. Gutkind and J. F. Rusling, *Biosens. Bioelectron.*, 2011, **26**, 4477–4483.
50 M. Mohammed and M. Desmulliez, *Biosens. Bioelectron.*, 2014, **61**, 478–484.

51 N. M. Matos Pires and T. Dong, *Sensors*, 2013, **13**, 15898–15911.
52 R. K. Jena, C. Yue and Y. Lam, *Microsys. Technol.*, 2012, **18**, 159–166.
53 H. Yu, S. Tor and N. Loh, *J. Micromech. Microeng.*, 2014, **24**, 115020.
54 M. Ornatska, E. Sharpe, D. Andreescu and S. Andreescu, *Anal. Chem.*, 2011, **83**, 4273–4280.
55 M. Su, L. Ge, S. Ge, N. Li, J. Yu, M. Yan and J. Huang, *Anal. Chim. Acta*, 2014, **847**, 1–9.
56 J. Hu, L. Wang, F. Li, Y. L. Han, M. Lin, T. J. Lu and F. Xu, *Lab Chip*, 2013, **13**, 4352–4357.
57 P. Liu, X. Li, S. A. Greenspoon, J. R. Scherer and R. A. Mathies, *Lab Chip*, 2011, **11**, 1041–1048.
58 X. Y. Liu, C. M. Cheng, A. W. Martinez, K. A. Mirica, X. J. Li, S. T. Phillips, M. Mascarenas and G. M. Whitesides, *Proc. IEEE Micr. Elect.*, 2011, 75–78.
59 X. Y. Liu, M. O'Brien, M. Mwangi, X. J. Li and G. M. Whitesides, *Proc. IEEE Micr. Elect.*, 2011, 133–136.
60 Y. L. Han, W. Wang, J. Hu, G. Huang, S. Wang, W. G. Lee, T. J. Lu and F. Xu, *Lab Chip*, 2013, **13**, 4745–4749.
61 S. Wang, F. Inci, T. L. Chaunzwa, A. Ramanujam, A. Vasudevan, S. Subramanian, A. C. F. Ip, B. Sridharan, U. A. Gurkan and U. Demirci, *Int. J. Nanomed.*, 2012, **7**, 2591.
62 J. F. Ashley, N. B. Cramer, R. H. Davis and C. N. Bowman, *Lab Chip*, 2011, **11**, 2772–2778.
63 N. S. G. K. Devaraju and M. A. Unger, *Lab Chip*, 2011, **11**, 1962–1967.
64 Y. Xia and G. M. Whitesides, *Annu. Rev. Mater. Sci.*, 1998, **28**, 153–184.
65 Z. Nie, C. A. Nijhuis, J. Gong, X. Chen, A. Kumachev, A. W. Martinez, M. Narovlyansky and G. M. Whitesides, *Lab Chip*, 2010, **10**, 477–483.
66 X. Liu, M. Mwangi, X. Li, M. O'Brien and G. M. Whitesides, *Lab Chip*, 2011, **11**, 2189–2196.
67 H. Becker and C. Gärtner, *Anal. Bioanal. Chem.*, 2008, **390**, 89–111.
68 A. K. Yetisen, M. S. Akram and C. R. Lowe, *Lab Chip*, 2013, **13**, 2210–2251.
69 E. Sollier, C. Murray, P. Maoddi and D. Di Carlo, *Lab Chip*, 2011, **11**, 3752–3765.
70 Y.-C. Kung, K.-W. Huang, Y.-J. Fan and P.-Y. Chiou, *Lab Chip*, 2015, **15**, 1861–1868.
71 D. Qin, Y. Xia and G. M. Whitesides, *Nat. Protoc.*, 2010, **5**, 491–502.
72 G. Comina, A. Suska and D. Filippini, *Lab Chip*, 2014, **14**, 424–430.
73 A. Rasooly, H. A. Bruck and Y. Kostov, in *Microfluidic Diagnostics*, Springer, 2013, pp. 451–471.
74 C. L. Cassano, A. J. Simon, W. Liu, C. Fredrickson and Z. H. Fan, *Lab Chip*, 2015, **15**, 62–66.
75 H. Becker and U. Heim, *Sens. Actuators, A*, 2000, **83**, 130–135.
76 D. Mathiesen and R. Dupaix, *in Challenges in Mechanics of Time-Dependent Materials*, Springer, 2015, vol. 2, pp. 73–80.
77 R. Suriano, A. Kuznetsov, S. M. Eaton, R. Kiyan, G. Cerullo, R. Osellame, B. N. Chichkov, M. Levi and S. Turri, *Appl. Surf. Sci.*, 2011, **257**, 6243–6250.
78 L. Zema, G. Loreti, A. Melocchi, A. Maroni and A. Gazzaniga, *J. Controlled Release*, 2012, **159**, 324–331.
79 E. Roy, J.-C. Galas and T. Veres, *Lab Chip*, 2011, **11**, 3193–3196.
80 S. Miserere, G. Mottet, V. Taniga, S. Descroix, J.-L. Viovy and L. Malaquin, *Lab Chip*, 2012, **12**, 1849–1856.
81 O. Rahmanian and D. L. DeVoe, *Lab Chip*, 2013, **13**, 1102–1108.
82 C.-S. Yang, C.-H. Lin, A. Zaytsev, K.-C. Teng, T.-H. Her and C.-L. Pan, *Appl. Phys. Lett.*, 2015, **106**, 051902.
83 Y. Lu, W. Shi, L. Jiang, J. Qin and B. Lin, *Electrophoresis*, 2009, **30**, 1497–1500.
84 X. Li, J. Tian, G. Garnier and W. Shen, *Colloids Surf., B*, 2010, **76**, 564–570.
85 A. W. Martinez, S. T. Phillips, M. J. Butte and G. M. Whitesides, *Angew. Chem., Int. Ed.*, 2007, **46**, 1318–1320.
86 A. W. Martinez, S. T. Phillips, B. J. Wiley, M. Gupta and G. M. Whitesides, *Lab Chip*, 2008, **8**, 2146–2150.
87 W. Dungchai, O. Chailapakul and C. S. Henry, *Analyst*, 2011, **136**, 77–82.
88 K.-F. Huang and Y.-C. Lee, *J. Vac. Sci. Technol., B*, 2013, **31**, 031604.
89 H. N. Chan, Y. Chen, Y. Shu, Y. Chen, Q. Tian and H. Wu, *Microfluid. Nanofluid.*, 2015, 1–10.
90 Q. He, C. Ma, X. Hu and H. Chen, *Anal. Chem.*, 2013, **85**, 1327–1331.
91 J. Olkkonen, K. Lehtinen and T. Erho, *Anal. Chem.*, 2010, **82**, 10246–10250.
92 T. Songjaroen, W. Dungchai, O. Chailapakul and W. Laiwattanapaisal, *Talanta*, 2011, **85**, 2587–2593.
93 E. Carrilho, A. W. Martinez and G. M. Whitesides, *Anal. Chem.*, 2009, **81**, 7091–7095.
94 Y. Sameenoi, P. N. Nongkai, S. Nouanthavong, C. S. Henry and D. Nacapricha, *Analyst*, 2014, **139**, 6580–6588.
95 P. Zuo, X. Li, D. C. Dominguez and B.-C. Ye, *Lab Chip*, 2013, **13**, 3921–3928.
96 E. Fu, B. Lutz, P. Kauffman and P. Yager, *Lab Chip*, 2010, **10**, 918–920.
97 M. M. Thuo, R. V. Martinez, W.-J. Lan, X. Liu, J. Barber, M. B. Atkinson, D. Bandarage, J.-F. Bloch and G. M. Whitesides, *Chem. Mater.*, 2014, **26**, 4230–4237.
98 D. Vilela, M. C. González and A. Escarpa, *Anal. Chim. Acta*, 2012, **751**, 24–43.
99 W. Qu, Y. Liu, D. Liu, Z. Wang and X. Jiang, *Angew. Chem., Int. Ed.*, 2011, **123**, 3504–3507.
100 L. Wu and X. Qu, *Chem. Soc. Rev.*, 2015, **44**, 2963–2997.

101 X. Li, D. R. Ballerini and W. Shen, *Biomicrofluidics*, 2012, **6**, 011301.
102 Z. Gao, M. Xu, M. Lu, G. Chen and D. Tang, *Biosens. Bioelectron.*, 2015, **70**, 194–201.
103 W.-F. Fang, W.-J. Chen and J.-T. Yang, *Sens. Actuators, B*, 2014, **192**, 77–82.
104 L. Yu, Y. Liu, Y. Gan and C. M. Li, *Biosens. Bioelectron.*, 2009, **24**, 2997–3002.
105 J. Park, V. Sunkara, T.-H. Kim, H. Hwang and Y.-K. Cho, *Anal. Chem.*, 2012, **84**, 2133–2140.
106 X. Fang, Y. Liu, J. Kong and X. Jiang, *Anal. Chem.*, 2010, **82**, 3002–3006.
107 W. Wang, W.-Y. Wu, W. Wang and J.-J. Zhu, *J. Chromatogr., A*, 2010, **1217**, 3896–3899.
108 H. A. Ahmed and H. M. Azzazy, *Biosens. Bioelectron.*, 2013, **49**, 478–484.
109 W. Dungchai, O. Chailapakul and C. S. Henry, *Anal. Chim. Acta*, 2010, **674**, 227–233.
110 K. F. Lei and Y. K. Butt, *Microfluid. Nanofluid.*, 2010, **8**, 131–137.
111 L. Liang, S. Ge, L. Li, F. Liu and J. Yu, *Anal. Chim. Acta*, 2015, **862**, 70–76.
112 A. Kumar, A. Hens, R. K. Arun, K. Mahato, M. Chatterjee, K. Layek and N. Chanda, *Analyst*, 2015, **140**, 1817–1821.
113 A. Baeissa, N. Dave, B. D. Smith and J. Liu, *ACS Appl. Mater. Interfaces*, 2010, **2**, 3594–3600.
114 C.-H. Wang, C.-J. Chang, J.-J. Wu and G.-B. Lee, *Nanomedicine*, 2014, **10**, 809–818.
115 A. H. Diercks, A. Ozinsky, C. L. Hansen, J. M. Spotts, D. J. Rodriguez and A. Aderem, *Anal. Biochem.*, 2009, **386**, 30–35.
116 V. Castro-López, J. Elizalde, M. Pacek, E. Hijona and L. Bujanda, *Biosens. Bioelectron.*, 2014, **54**, 499–505.
117 X. Wang, M. J. Theodore, R. Mair, E. Trujillo-Lopez, M. du Plessis, N. Wolter, A. L. Baughman, C. Hatcher, J. Vuong and L. Lott, *J. Clin. Microbiol.*, 2012, **50**, 702–708.
118 W. Jing, W. Zhao, S. Liu, L. Li, C.-T. Tsai, X. Fan, W. Wu, J. Li, X. Yang and G. Sui, *Anal. Chem.*, 2013, **85**, 5255–5262.
119 H. N. Joensson, M. L. Samuels, E. R. Brouzes, M. Medkova, M. Uhlén, D. R. Link and H. Andersson-Svahn, *Angew. Chem., Int. Ed.*, 2009, **48**, 2518–2521.
120 Y.-H. Lin, C.-C. Wang and K. F. Lei, *Biomed. Microdev.*, 2014, **16**, 199–207.
121 R. Riahi, P. Gogoi, S. Sepehri, Y. Zhou, K. Handique, J. Godsey and Y. Wang, *Int. J. Oncol.*, 2014, **44**, 1870–1878.
122 M. Hu, J. Yan, Y. He, H. Lu, L. Weng, S. Song, C. Fan and L. Wang, *ACS Nano*, 2009, **4**, 488–494.
123 H. Zhang, L. Liu, X. Fu and Z. Zhu, *Biosens. Bioelectron.*, 2013, **42**, 23–30.
124 X. Yu, H.-S. Xia, Z.-D. Sun, Y. Lin, K. Wang, J. Yu, H. Tang, D.-W. Pang and Z.-L. Zhang, *Biosens. Bioelectron.*, 2013, **41**, 129–136.
125 J. M. Hoffman, P. S. Stayton, A. S. Hoffman and J. J. Lai, *Bioconjugate Chem.*, 2014, **26**(1), 29–38.
126 E. J. Maxwell, A. D. Mazzeo and G. M. Whitesides, *MRS Bull.*, 2013, **38**, 309–314.
127 M. U. Ahmed, M. M. Hossain, M. Safavieh, Y. L. Wong, I. A. Rahman, M. Zourob and E. Tamiya, *Crit. Rev. Biotechnol.*, 2015, 1–11.
128 W. Su, X. Gao, L. Jiang and J. Qin, *J. Chromatogr., A*, 2014, **1377**, 13–26.
129 B. V. Chikkaveeraiah, A. A. Bhirde, N. Y. Morgan, H. S. Eden and X. Chen, *ACS Nano*, 2012, **6**, 6546–6561.
130 X. Li, Z. Nie, C. Cheng, A. Goodale and G. Whitesides, *Proc. Micro Total Analysis Systems*, 2010, **14**, 1487–1489.
131 G. Sun, Y.-n. Ding, C. Ma, Y. Zhang, S. Ge, J. Yu and X. Song, *Electrochim. Acta*, 2014, **147**, 650–656.
132 Y. Bai, C. G. Koh, M. Boreman, Y.-J. Juang, I.-C. Tang, L. J. Lee and S.-T. Yang, *Langmuir*, 2006, **22**, 9458–9467.
133 Y. Liu, H. Wang, J. Huang, J. Yang, B. Liu and P. Yang, *Anal. Chim. Acta*, 2009, **650**, 77–82.
134 F. Zhou, M. Lu, W. Wang, Z.-P. Bian, J.-R. Zhang and J.-J. Zhu, *Clin. Chem.*, 2010, **56**, 1701–1707.
135 W. Liang, Y. Li, B. Zhang, Z. Zhang, A. Chen, D. Qi, W. Yi and C. Hu, *Biosens. Bioelectron.*, 2012, **31**, 480–485.
136 C. Zhao, M. M. Thuo and X. Liu, *Sci. Tech. Adv. Mater.*, 2013, **14**, 054402.
137 H. Ben-Yoav, P. H. Dykstra, W. E. Bentley and R. Ghodssi, *Biosens. Bioelectron.*, 2015, **64**, 579–585.
138 M. Iranifam, *TrAC, Trends Anal. Chem.*, 2014, **59**, 156–183.
139 N. M. M. Pires, T. Dong, U. Hanke and N. Hoivik, *Sensors*, 2014, **14**, 15458–15479.
140 L. Ge, S. Wang, X. Song, S. Ge and J. Yu, *Lab Chip*, 2012, **12**, 3150–3158.
141 N. M. M. Pires, T. Dong, U. Hanke and N. Hoivik, *J. Biomed. Opt.*, 2013, **18**, 097001–097001.
142 W. Liu, H. Wei, Z. Lin, S. Mao and J.-M. Lin, *Biosens. Bioelectron.*, 2011, **28**, 438–442.
143 M. Yang, Y. Kostov, H. A. Bruck and A. Rasooly, *Int. J. Food Microbiol.*, 2009, **133**, 265–271.
144 X. Zhao and T. Dong, *Sensors*, 2013, **13**, 14570–14582.
145 L. Hu and G. Xu, *Chem. Soc. Rev.*, 2010, **39**, 3275–3304.
146 W. K. Tomazelli Coltro, C. M. Cheng, E. Carrilho and D. P. Jesus, *Electrophoresis*, 2014, **35**, 2309–2324.
147 L. Ge, J. Yan, X. Song, M. Yan, S. Ge and J. Yu, *Biomaterials*, 2012, **33**, 1024–1031.
148 H. Yang, Q. Kong, S. Wang, J. Xu, Z. Bian, X. Zheng, C. Ma, S. Ge and J. Yu, *Biosens. Bioelectron.*, 2014, **61**, 21–27.
149 Y. Qi and B. Li, *Chem. – Eur. J.*, 2011, **17**, 1642–1648.
150 Y. Xu, B. Lou, Z. Lv, Z. Zhou, L. Zhang and E. Wang, *Anal. Chim. Acta*, 2013, **763**, 20–27.
151 M. Li, Y. Wang, Y. Zhang, J. Yu, S. Ge and M. Yan, *Biosens. Bioelectron.*, 2014, **59**, 307–313.
152 Y. Koh, B.-R. Lee, H.-J. Yoon, Y.-H. Jang, Y.-S. Lee, Y.-K. Kim and B.-G. Kim, *Anal. Bioanal. Chem.*, 2012, **404**, 2267–2275.

153 M. Z. Mousavi, H.-Y. Chen, K.-L. Lee, H. Lin, H.-H. Chen, Y.-F. Lin, C. S. Wong, H.-F. Li, P.-K. Wei and J.-Y. Cheng, *Analyst*, 2015, **140**, 4097–4104.
154 L. Tian, J. J. Morrissey, R. Kattumenu, N. Gandra, E. D. Kharasch and S. Singamaneni, *Anal. Chem.*, 2012, **84**, 9928–9934.
155 X. Xu, A. Akay, H. Wei, S. Wang, B. Pingguan-Murphy, B.-E. Erlandsson, X. Li, W. Lee, J. Hu and L. Wang, *Proc. IEEE*, 2015, **103**, 236–247.
156 T. Laksanasopin, T. W. Guo, S. Nayak, A. A. Sridhara, S. Xie, O. O. Olowookere, P. Cadinu, F. Meng, N. H. Chee and J. Kim, *Sci. Transl. Med.*, 2015, **7**, 273re271–273re271.
157 B. S. Lee, Y. U. Lee, H.-S. Kim, T.-H. Kim, J. Park, J.-G. Lee, J. Kim, H. Kim, W. G. Lee and Y.-K. Cho, *Lab Chip*, 2011, **11**, 70–78.
158 J. Nguyen, Y. Wei, Y. Zheng, C. Wang and Y. Sun, *Lab Chip*, 2015, **15**, 1533–1544.